Electronic Supplementary Information

Revisiting the Juliá-Colonna enantioselective epoxidation: supramolecular catalysis in water

Christopher Bérubé[1], Xavier Barbeau[2], Patrick Lagüe[2] and Normand Voyer[1]

[1]Département de Chimie and PROTEO, Université Laval, Pavillon Alexandre-Vachon, Faculté des sciences et de génie, 1045 avenue de la Médecine, Québec, QC, Canada, G1V 0A6

E-mail : normand.voyer@chm.ulaval.ca

[2]Département de biochimie, microbiologie et bioinformatique and PROTEO, Université Laval, Faculté des sciences et de génie, 1030 avenue de la Médecine, Québec, QC, G1V OA6

Table of contents

General information:

1,3-diaminopropane-poly-L-Leucine (DAP-PLL) was purchased from AcrosOrganics. All chemicals were purchased from commercial sources and used directly, unless indicated otherwise. Nuclear magnetic resonance (NMR) spectra were recorded using Varian Inova 400 MHz and NMR Agilent DD2 500 MHz spectrometers. The coupling constants are reported in hertz (Hz). Chemical shifts are reported in parts per million downfield from TMS. Splitting patterns are designated as s (singlet), d (doublet), dd (doublet of doublets), t (triplet), q (quartet), br (broad singlet) and m (multiplet). MALDI-TOF spectra were obtained on an AXIMA Assurance Linear mass spectrometer. Polymerization degree were calculated using Shimadzu software. Optical rotations were measured at ambient temperature on a Jasco DIP-360 digital polarimeter using a sodium lamp. IR spectra were recorded on a Thermo Scientific Nicolet iS50 ATR spectrometer using diamond as crystal.

Preparation of starting material

General procedures

General procedure for the synthesis of non-commercial α,β-unsaturated ketones via Claisen-Schmidt conditions[1]

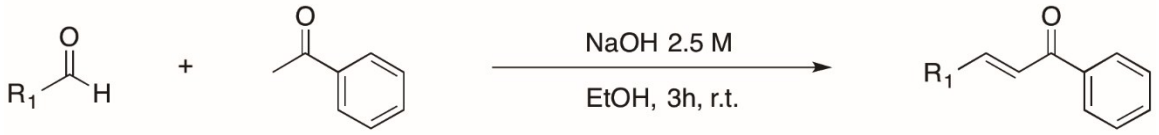

To a solution of substituted ketone in ethanol was added the corresponding substituted aldehyde and sodium hydroxide (2.5 M) at room temperature. The mixture was stirred for 3 h, neutralized with HCl 2M and extracted with AcOEt. The organic layer was dried with Na_2SO_4 and evaporated. If necessary, the residue was purified by a simple trituration using a small amount of cold hexanes.

3-(4-trifluoromethylphenyl)-1-phenylpro-2-en-1-one[2]

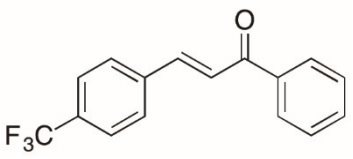

80% yield, yellow powder; **^{1}H NMR** (400 MHz, $CDCl_3$): δ = 7.52 (t, *J* = 7.6 Hz, 2H), 7.58-7.64 (m, 2H), 7.67 (d, *J* = 8.3 Hz, 2H), 7.74 (d, *J* = 8.2 Hz, 2H), 7.81 (d, *J* = 15.7 Hz, 1H), 8.02-8.04 (m, 2H). **^{13}C NMR** (101 MHz, $CDCl_3$): δ = 124.2, 125.8, 125.9 (q, 3.8 Hz), 133.1, 137.8, 138.2, 142.7, 190.0. **^{19}F NMR** (75 MHz, $CDCl_3$): δ = -62.85.

3-(4-naphthalen-2-yl)-1-phenylpro-2-en-1-one[2]

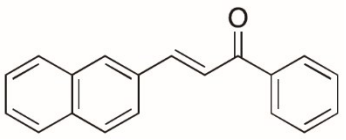

87% yield, yellow powder; **^{1}H NMR** (400 MHz, $CDCl_3$): δ = 7.51-7.56 (m, 4H), 7.59-7.63 (m, 1H), 7.65 (d, *J* = 15.7 Hz, 1H), 7.80 (dd, *J* = 8.6, 1.8 Hz, 1H), 7.84-7.90 (m, 3H), 7.99 (d, *J* = 15.7 Hz, 1H), 8.02-8.09 (m, 3H). **^{13}C NMR** (101 MHz, $CDCl_3$): δ = 122.2, 123.7, 126.8, 127.4, 127.8, 128.5, 128.6, 128.7, 130.6, 132.4, 132.8, 133.4, 134.4, 138.3, 144.9, 190.5.

Preparation of homo-oligopeptide catalysts[3]

General procedure for the synthesis of N-carboxyanhydrides

Amino acid and charcoal (0.02 m/m from the starting amino acid) were dried under reduced pressure for 30 min. Then, they were poured in a flask under argon with freshly distilled THF (80 mL). Diphosgene (2.8 mL) was added slowly and the reaction mixture was allowed to warm at 49 ^{o}C and stirred for 1.5 h. Temperature was cooled down to room temperature and filtered two times on a Celite® pad and washed with Et_2O (300 mL). The filtrate was concentrated *in vacuo*. A small amount of hexanes was then added to precipitate the product, yielding to the corresponding *N*-carboxyanhydride described below.

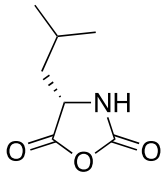

(S)-4-isobutyloxazolidine-2,5-dione.[3-4] White powder (3.50g, 73% yield). **^{1}H NMR** (400 MHz, $CDCl_3$): δ = 0.98 (dd, *J* = 8.7, 6.2, 6H), 1.64-1.73 (m, 1H), 1.77-1.85 (m, 2H), 4.35 (dd, *J* = 9.0, 4.1, 1H), 7.15 (s, 1H). **^{13}C NMR** (101 MHz, $CDCl_3$): δ = 21.5, 22.7, 25.0, 40.8, 56.2, 153.2, 170.0.

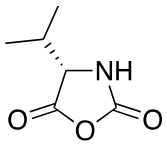

(S)-4-((S)-sec-butyl)oxazolidine-2,5-dione.[4] Pale green powder (1.13g, 95% yield). **^{1}H NMR** (400 MHz, DMSO-d_6): δ = 0.74-0.93 (m, 6H), 1.12-1.33 (m, 2H), 1.74 (s, 1H), 4.34 (s, 1H), 9.04 (s, 1H). **^{13}C NMR** (101 MHz, DMSO-d_6): δ = 11.7, 15.1, 24.2, 36.9, 62.1, 152.6, 171.2.

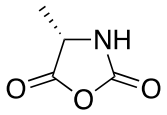

(S)-4-methyloxazolidine-2,5-dione.[4] Beige powder (1.07g, 81% yield). **^{1}H NMR** (400 MHz, DMSO-d_6): δ = 1.28 (d, *J* = 6.9 Hz, 3H), 4.42 (q, *J* = 6.9 Hz, 1H), 8.95 (s, 1H). **^{13}C NMR** (101 MHz, DMSO-d_6): δ = 17.2, 53.2, 152.1, 172.8.

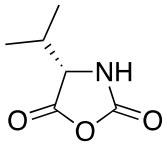

(S)-4-isopropyloxazolidine-2,5-dione.[4] Brown powder (1.13g, 93% yield). **^{1}H NMR** (400 MHz, DMSO-d_6): δ = 0.81 (d, *J* = 6.7 Hz, 3H), 0.90 (d, *J* = 6.8 Hz, 3H), 1.88-2.16 (m, 1H), 4.29 (d, *J* = 3.9 Hz, 1H), 9.05 (s, 1H). **^{13}C NMR** (101 MHz, DMSO-d_6): δ = 16.8, 18.5, 30.3, 62.8, 152.7, 171.3.

General procedure for the polymerisation of N-Carboxyanhydrides

In a round-bottom flask, *N*-Carboxyanhydride (1.0 equiv.) was dissolved in freshly distilled THF under argon. Freshly distilled 1,3-diaminopropane (0.0018 equiv.) was then added and the reaction mixture was stirred at room temperature for 72 h. The precipitate was filtered and washed with a minimum of Et_2O. The solid was dried under vacuum pulverised into fine powder, giving 2.32 g, 0.560 g, 0.470 g and 0.367 g of PLL, PLA, PLI and PLV respectively as white powders. Homo-oligopeptides are insoluble in water and all common organic solvents. MALDI-TOF spectra were done in trifluoroacetic acid, in which they are all soluble. Using MALDI-TOF mass spectrometry, we observed homo-oligopeptides containing on average approximately 1500-4000 g/mol, in agreement with the literature.[3]

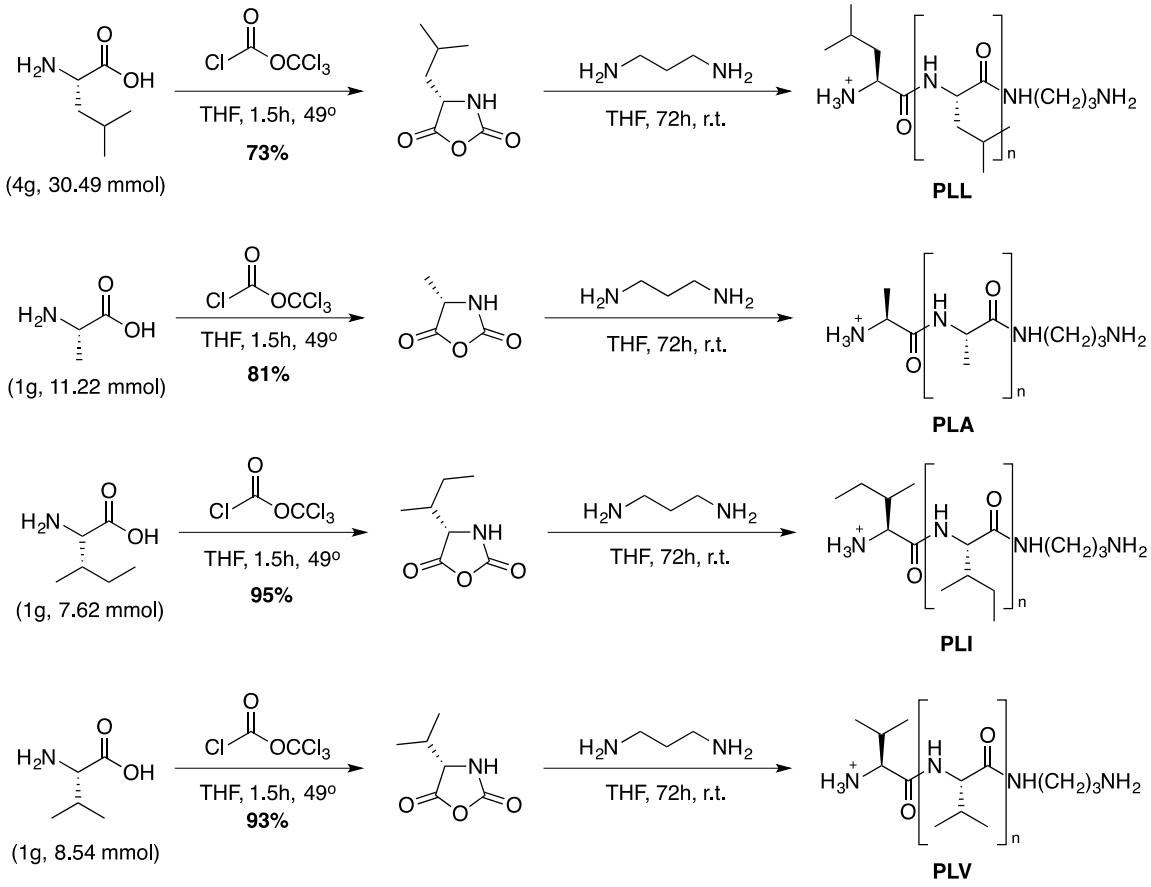

Commercial poly-L-leucine (DAP-PLL) MALDI-TOF spectrum

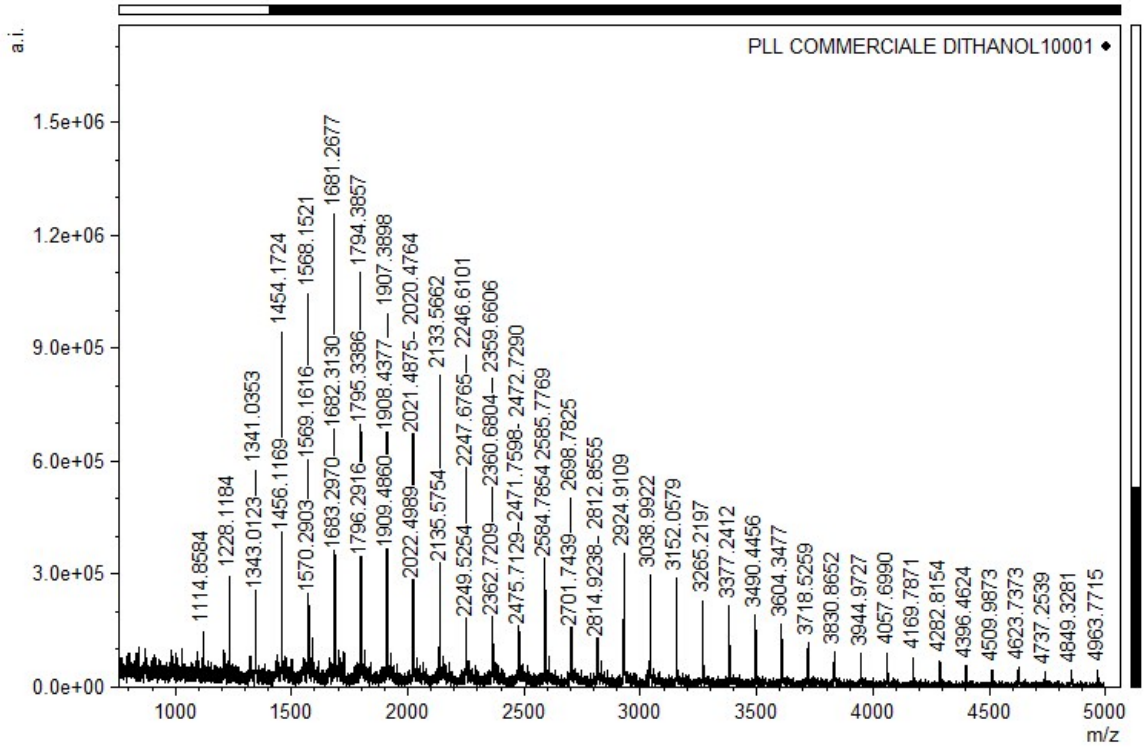

Synthetic poly-L-leucine (PLL) MALDI-TOF spectrum

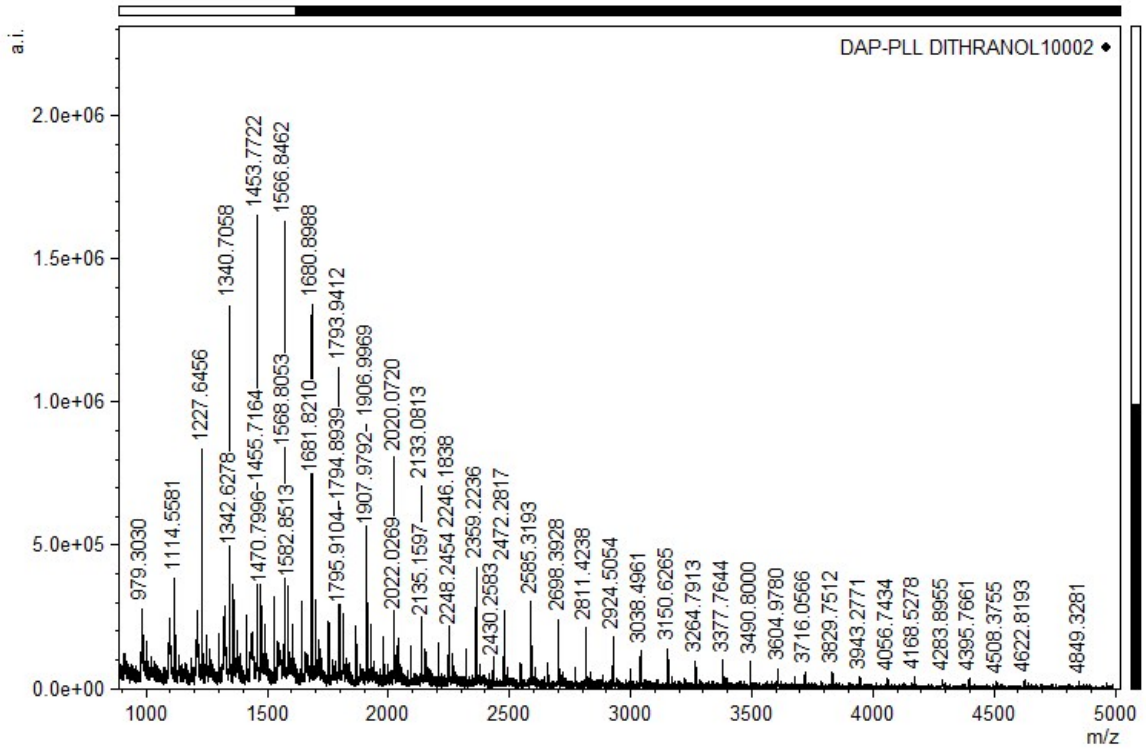

Synthetic poly-L-Alanine (PLA) MALDI-TOF spectrum

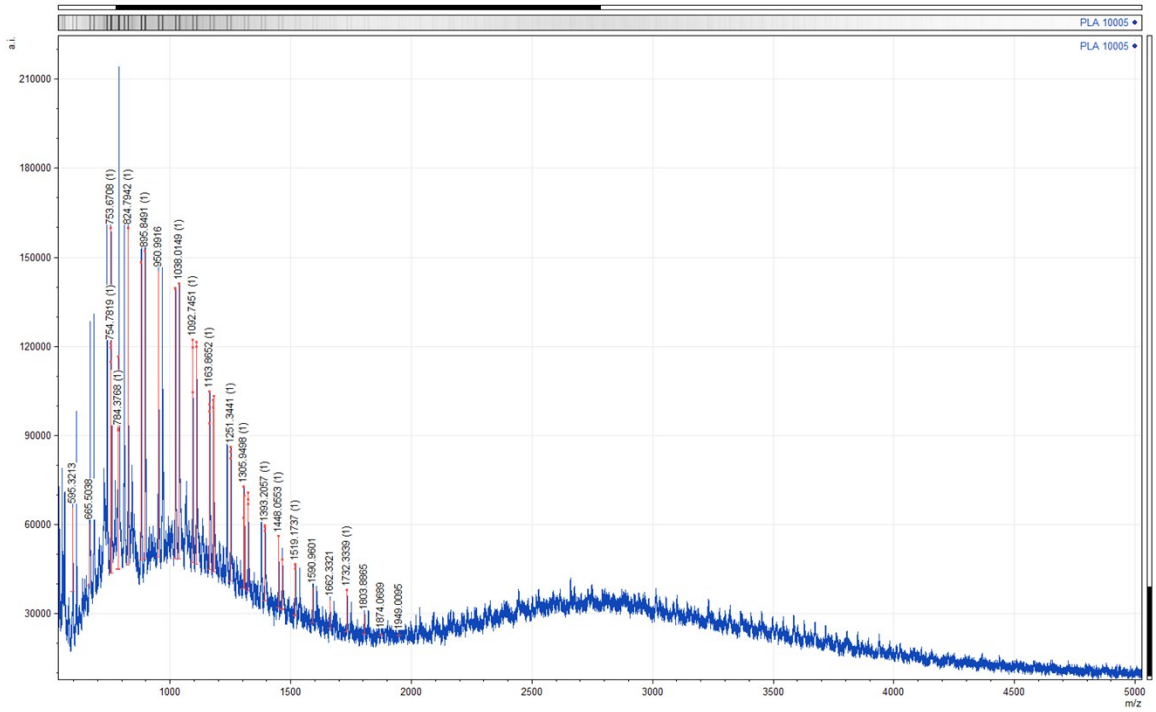

Synthetic poly-L-Isoleucine (PLI) MALDI-TOF spectrum

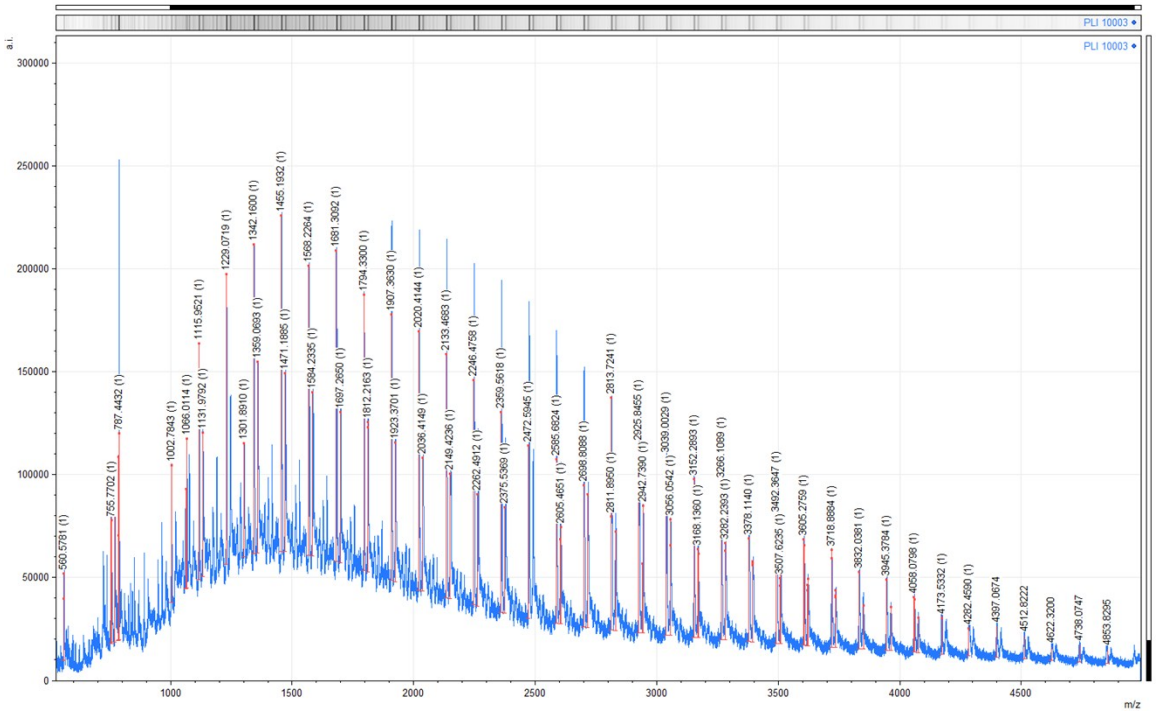

Synthetic poly-L-Valine (PLV) MALDI-TOF spectrum

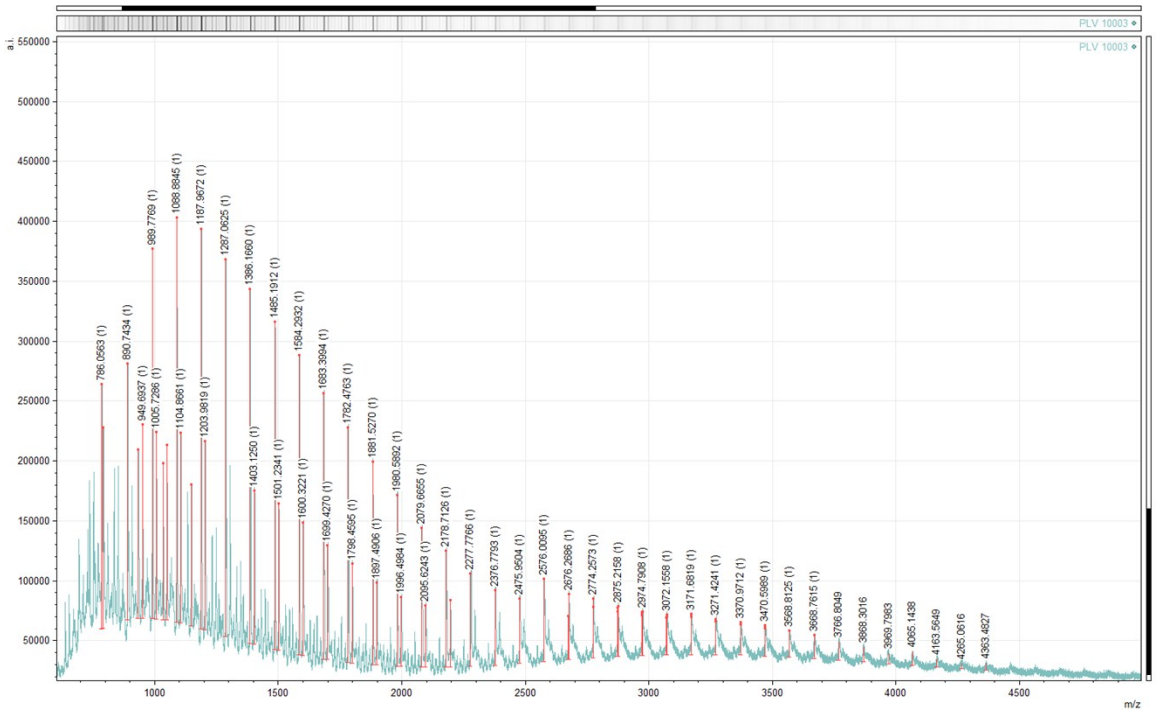

PLL polymerization degree calculated by MALDI-TOF Shimadzu software

Assurance

Data: PLL COMMERCIALE DITHANOL10001.A6[c] 11 Aug 2015 10:29 Cal: christopher11.08.15 11 Aug 2015 10:16
Shimadzu Biotech Axima Assurance 2.9.3.20110624: Mode Linear, Power: 100, P.Ext. @ 2500 (bin 75)
Cutoff: 1% Tolerance: 50 Da Averaged masses

Basic Statistics	Distribution: 1	Distribution: 2	Distribution: 3
Mass range:	436 - 4963	452 - 4759	414 - 3759
Peaks:	41	37	30
Area (mV):	239023	230273	226394
% Total area:	9.5195	9.1710	9.0165
Average mass:	2123.8887	2139.9229	2003.8541
Spread of mass:	4509.7051	4283.4136	3264.9391
Monomer mass:	112.8968	116.4605	112.8829
Sigma Monomer:	10.7481	19.3691	12.6180
Residual mass:	-10.4492	20.4874	-10.4311
Sigma Residual:	6.9993	44.4745	7.8153
Weight Averages Residue excluded			
DPn:	18.9052	18.1987	17.8440
DPw:	22.3979	21.2665	20.5215
DPz:	25.4369	24.0473	22.5468
Mn:	2134.3379	2119.4355	2014.2852
Mw:	2528.6516	2476.7057	2316.5308
Mz:	2871.7479	2800.5633	2545.1454
Polydispersity (Mw/Mn):	1.1847	1.1686	1.1501
Mass = m * Monomers + c			
LSQ fit m:	113.05805525	116.03279756	112.95653562
LSQ fit c:	-13.21227951	10.87537892	-11.67977550
LSQ Correl coeff:	0.99998733	0.99936305	0.99996826
Weight Averages Residue included			
DPn:	18.8127	18.3747	17.7516
DPw:	22.3252	21.4319	20.4419
DPz:	25.3871	24.0467	22.4815
Mn:	2123.8887	2139.9229	2003.8541
Mw:	2520.4414	2495.9746	2307.5401
Mz:	2866.1226	2800.4952	2537.7797
Polydispersity (Mw/Mn):	1.1867	1.1664	1.1516
Mass = m * Monomers + c			
LSQ fit m:	112.89680672	116.46050593	112.88290242
LSQ fit c:	-0.00000000	-0.00000000	0.00000000
LSQ Correl coeff:	1.00000000	1.00000000	1.00000000

PLA polymerization degree calculated by MALDI-TOF Shimadzu software

Assurance

Data: PLA 10001.K3[c] 1 Jun 2016 15:23 Cal: 2016.05.18 18 May 2016 11:01
Shimadzu Biotech Axima Assurance 2.9.3.20110624: Mode Linear, Power: 140, P.Ext. @ 2500 (bin 75)
Cutoff: 1% Tolerance: 50 Da Averaged masses

Basic Statistics	Distribution: 1	Distribution: 2	Distribution: 3
Mass range:	436 - 4963	452 - 4759	414 - 3759
Peaks:	37	44	22
Area (mV):	10097	16928	7946
% Total area:	4.2705	7.1599	3.3606
Average mass:	2259.3152	1716.3790	1744.7930
Spread of mass:	4444.7359	4169.2878	3288.7816
Monomer mass:	129.7562	92.8390	147.7639
Sigma Monomer:	27.0286	32.3272	29.4509
Residual mass:	-113.1639	85.5668	71.6842
Sigma Residual:	91.3625	116.4060	64.7764
Weight Averages Residue excluded			
DPn:	18.2841	17.5660	11.3228
DPw:	25.4160	28.7738	16.6575
DPz:	28.6466	34.3102	19.0083
Mn:	2372.4790	1630.8122	1673.1088
Mw:	3297.8836	2671.3333	2461.3706
Mz:	3717.0696	3185.3219	2808.7351
Polydispersity (Mw/Mn):	1.3901	1.6380	1.4711
Mass = m * Monomers + c			
LSQ fit m:	121.81317955	100.96167942	156.00574629
LSQ fit c:	41.11854530	-99.45594731	-11.04166012
LSQ Correl coeff:	0.99965885	0.99911556	0.99925466
Weight Averages Residue included			
DPn:	17.4120	18.4877	11.8080
DPw:	24.0513	30.7784	17.5842
DPz:	27.1887	36.6113	19.9522
Mn:	2259.3152	1716.3790	1744.7930
Mw:	3120.8100	2857.4330	2598.3131
Mz:	3527.8982	3398.9539	2948.2121
Polydispersity (Mw/Mn):	1.3813	1.6648	1.4892
Mass = m * Monomers + c			
LSQ fit m:	129.75616131	92.83895800	147.76393557
LSQ fit c:	0.00000000	0.00000000	0.00000000
LSQ Correl coeff:	1.00000000	1.00000000	1.00000000

PLI polymerization degree calculated by MALDI-TOF Shimadzu software

Assurance

Data: PLI 10003.I2[c] 1 Jun 2016 15:16 Cal: 2016.05.18 18 May 2016 11:01
Shimadzu Biotech Axima Assurance 2.9.3.20110624: Mode Linear, Power: 120, P.Ext. @ 2500 (bin 75)
Cutoff: 1% Tolerance: 50 Da Averaged masses

Basic Statistics	Distribution: 1	Distribution: 2	Distribution: 3
Mass range:	436 - 4963	452 - 4759	414 - 3759
Peaks:	40	40	29
Area (mV):	45297	46306	43243
% Total area:	6.8026	6.9540	6.4940
Average mass:	1904.1507	1881.7701	1859.4714
Spread of mass:	4394.4085	4284.5708	3262.2487
Monomer mass:	111.9785	108.8541	115.5720
Sigma Monomer:	3.7150	11.3089	12.8681
Residual mass:	10.1173	-18.9098	37.9900
Sigma Residual:	12.8636	39.2083	27.2488
Weight Averages Residue excluded			
DPn:	16.9143	17.4608	15.7606
DPw:	21.7941	22.4495	20.0989
DPz:	24.8633	25.5100	22.6998
Mn:	1894.0334	1900.6799	1821.4814
Mw:	2440.4761	2443.7241	2322.8650
Mz:	2784.1580	2776.8659	2623.4608
Polydispersity (Mw/Mn):	1.2885	1.2857	1.2753
Mass = m * Monomers + c			
LSQ fit m:	113.01781406	110.64952434	116.28302465
LSQ fit c:	-8.60625159	-47.21309171	24.64910400
LSQ Correl coeff:	0.99999367	0.99966066	0.99962668
Weight Averages Residue included			
DPn:	17.0046	17.2871	16.0893
DPw:	21.9106	22.3114	20.4318
DPz:	25.0250	25.5448	22.9610
Mn:	1904.1507	1881.7701	1859.4714
Mw:	2453.5166	2428.6844	2361.3391
Mz:	2802.2668	2780.6564	2653.6514
Polydispersity (Mw/Mn):	1.2885	1.2906	1.2699
Mass = m * Monomers + c			
LSQ fit m:	111.97853877	108.85414786	115.57196557
LSQ fit c:	0.00000000	0.00000000	0.00000000
LSQ Correl coeff:	1.00000000	1.00000000	1.00000000

PLV polymerization degree calculated by MALDI-TOF Shimadzu software

Assurance

Data: PLV 10002.M2[c] 1 Jun 2016 15:29 Cal: 2016.05.18 18 May 2016 11:01
Shimadzu Biotech Axima Assurance 2.9.3.20110624: Mode Linear, Power: 140, P.Ext. @ 2500 (bin 75)
Cutoff: 1% Tolerance: 50 Da Averaged masses

Basic Statistics	Distribution: 1	Distribution: 2	Distribution: 3
Mass range:	436 - 4963	452 - 4759	414 - 3759
Peaks:	46	43	17
Area (mV):	23178	22025	11776
% Total area:	7.7654	7.3792	3.9453
Average mass:	1598.7553	1620.9081	1360.4270
Spread of mass:	4445.1691	4250.9222	3092.1593
Monomer mass:	97.1612	101.2789	190.5199
Sigma Monomer:	18.4403	16.6844	14.9348
Residual mass:	36.0361	-32.4331	-120.7531
Sigma Residual:	26.4717	31.3469	33.2755
Weight Averages Residue excluded			
DPn:	16.0838	16.3246	7.7744
DPw:	22.6964	22.2423	9.9748
DPz:	28.9809	27.9448	11.9781
Mn:	1562.7191	1653.3411	1481.1800
Mw:	2205.2058	2252.6748	1900.3962
Mz:	2815.8138	2830.2184	2282.0627
Polydispersity (Mw/Mn):	1.4111	1.3625	1.2830
Mass = m * Monomers + c			
LSQ fit m:	98.73983866	99.34439486	196.14570541
LSQ fit c:	13.02829865	-0.54898889	-168.75859307
LSQ Correl coeff:	0.99992392	0.99986636	0.99981179
Weight Averages Residue included			
DPn:	16.4547	16.0044	7.1406
DPw:	23.1101	21.7737	9.6070
DPz:	29.5373	27.4034	11.8166
Mn:	1598.7553	1620.9081	1360.4270
Mw:	2245.4070	2205.2138	1830.3261
Mz:	2869.8823	2775.3817	2251.2890
Polydispersity (Mw/Mn):	1.4045	1.3605	1.3454
Mass = m * Monomers + c			
LSQ fit m:	97.16116533	101.27890191	190.51988073
LSQ fit c:	-0.00000000	-0.00000000	0.00000000
LSQ Correl coeff:	1.00000000	1.00000000	1.00000000

^{1}H-NMR spectrum of PLA in $CDCl_3$/TFA

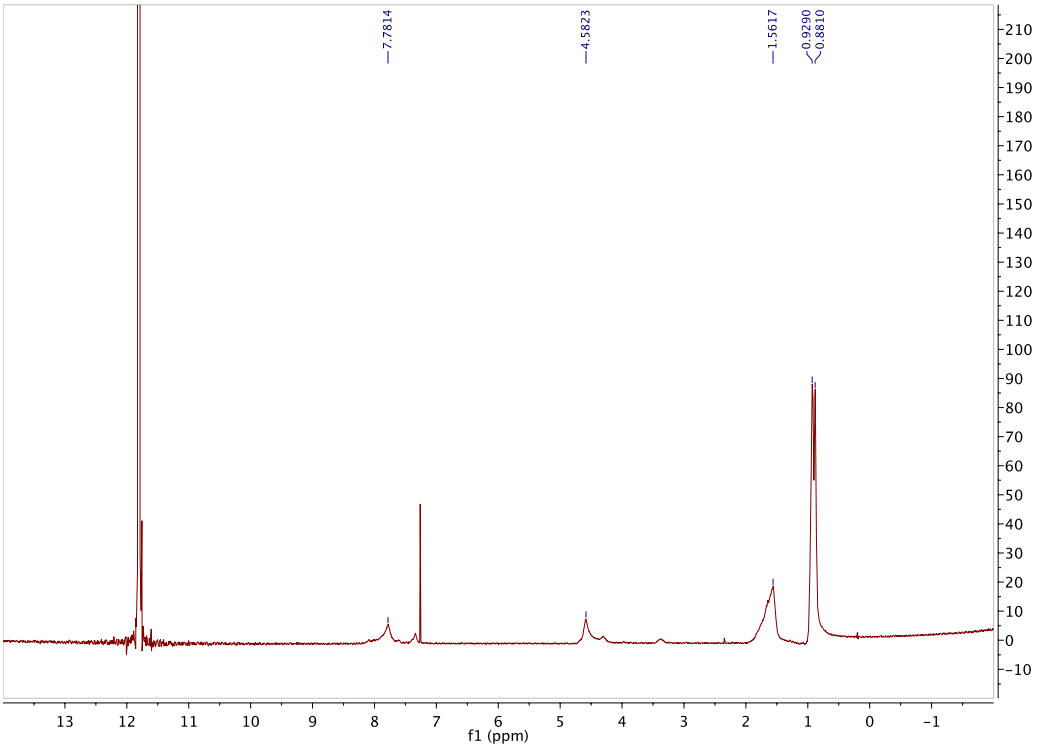

^{1}H-NMR spectrum of PLA in $CDCl_3$/TFA

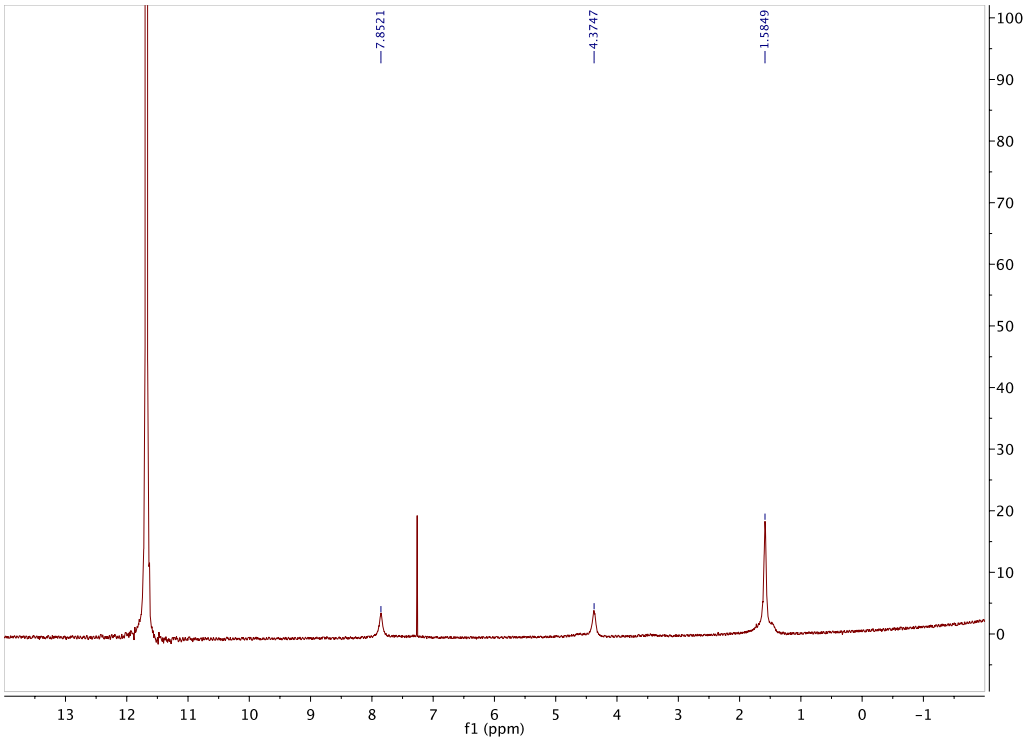

^{1}H-NMR spectrum of PLI in $CDCl_3$/TFA

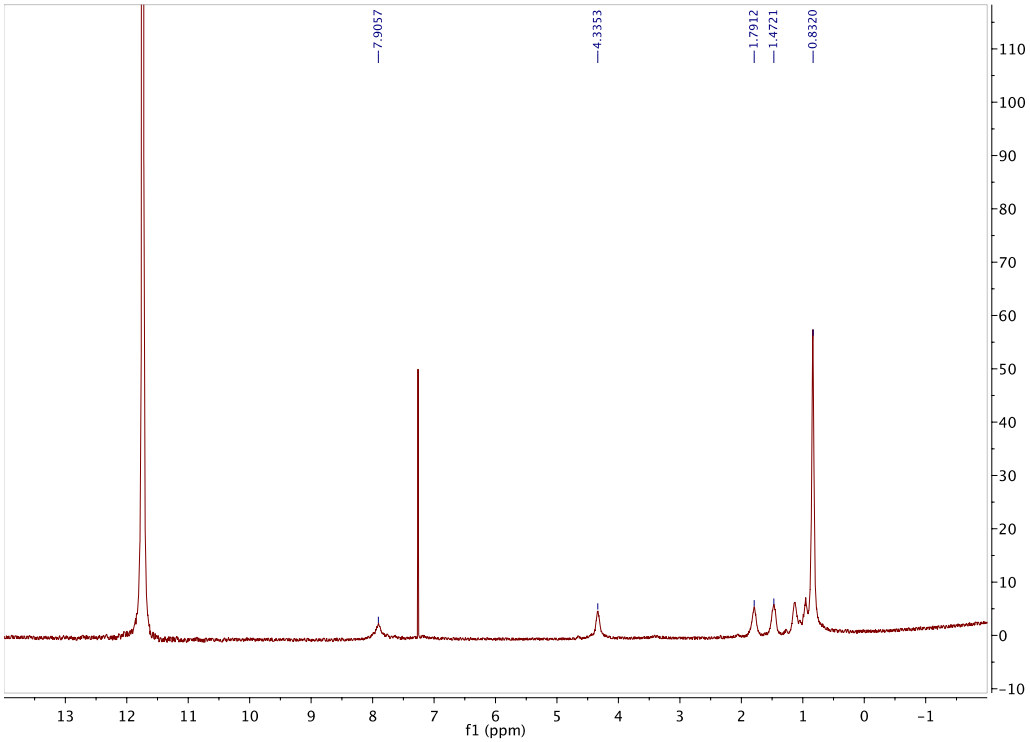

^{1}H-NMR spectrum of PLV in $CDCl_3$/TFA

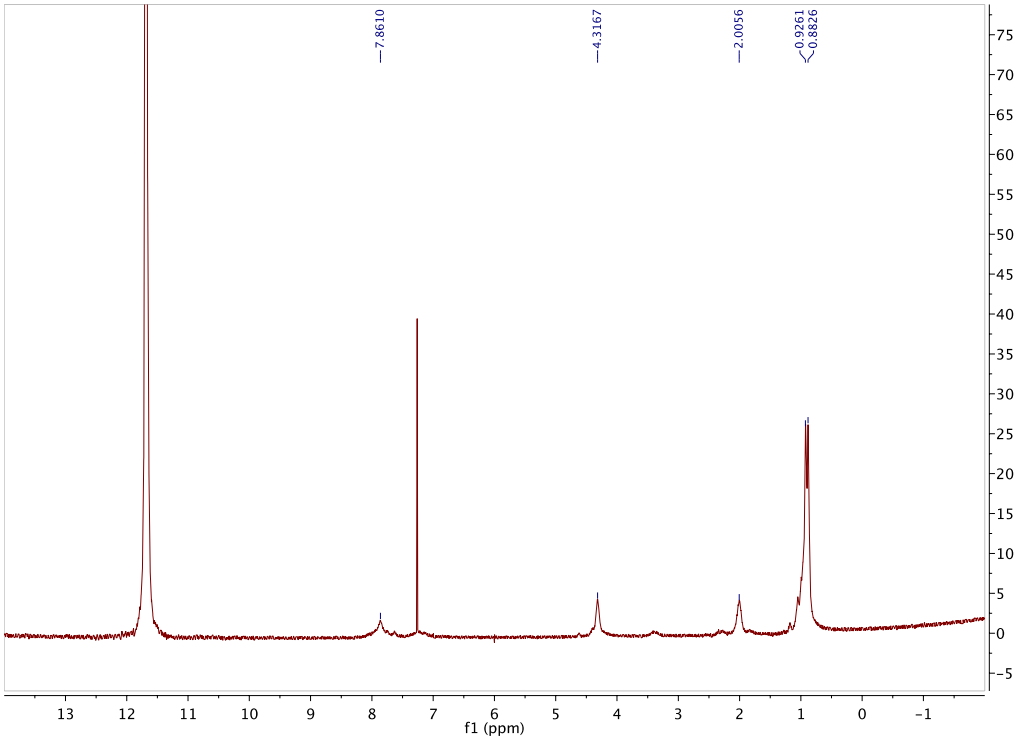

ATR-FTIR sprectra of homo-oligopeptide catalysts

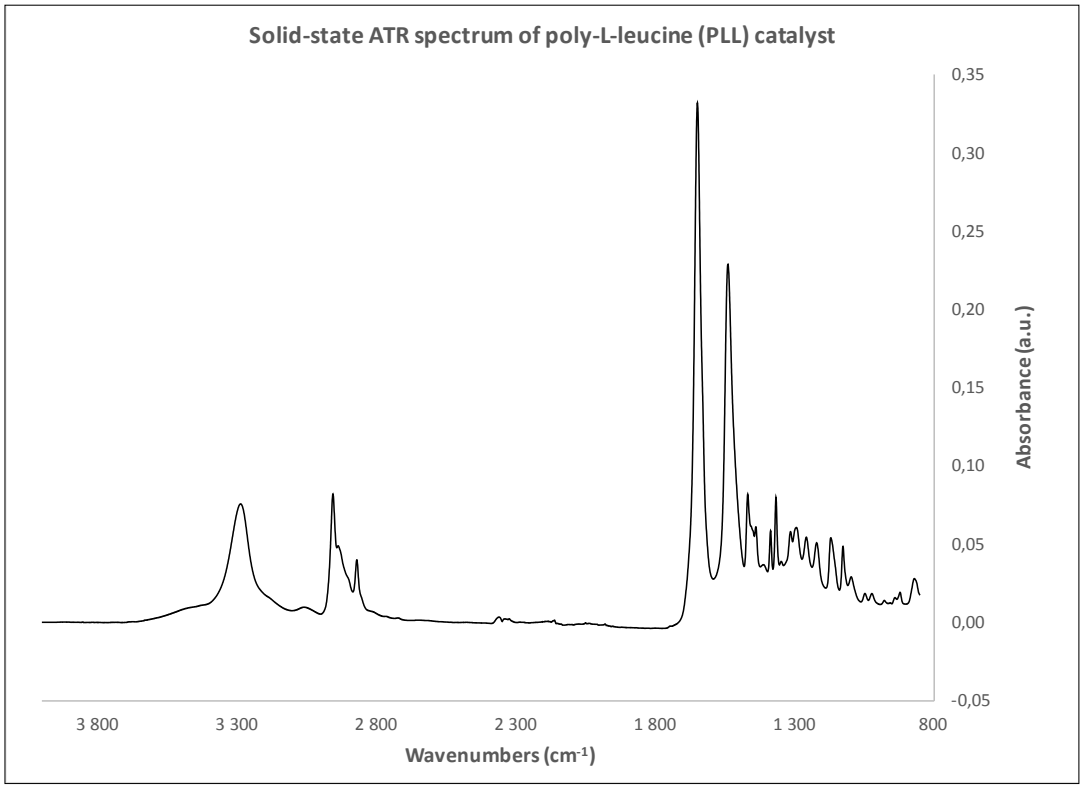

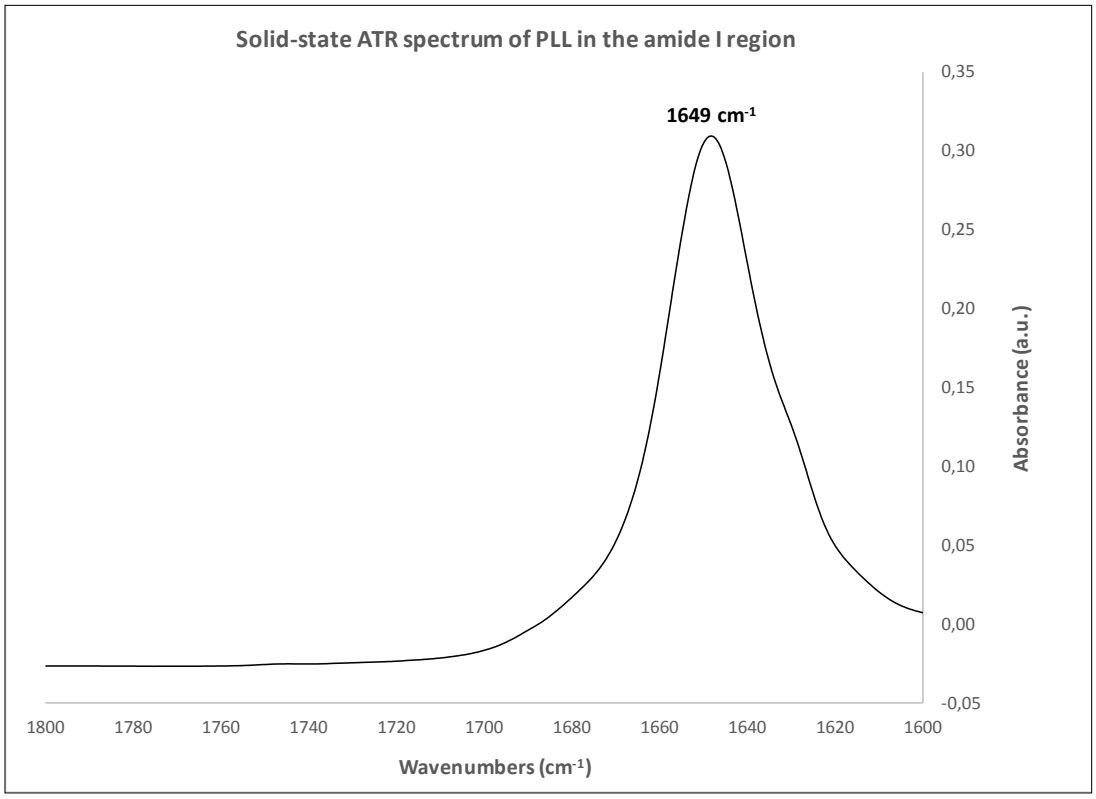
Solid-state ATR spectrum of PLL in the amide I region
1649 cm-1
0,35
0,30
0,25
0,20
0,15
0,10
0,05
0,00
-0,05
Absorbance (a.u.)
1800
1780
1760
1740
1720
1700
1680
1660
1640
1620
1600
Wavenumbers (cm-1)

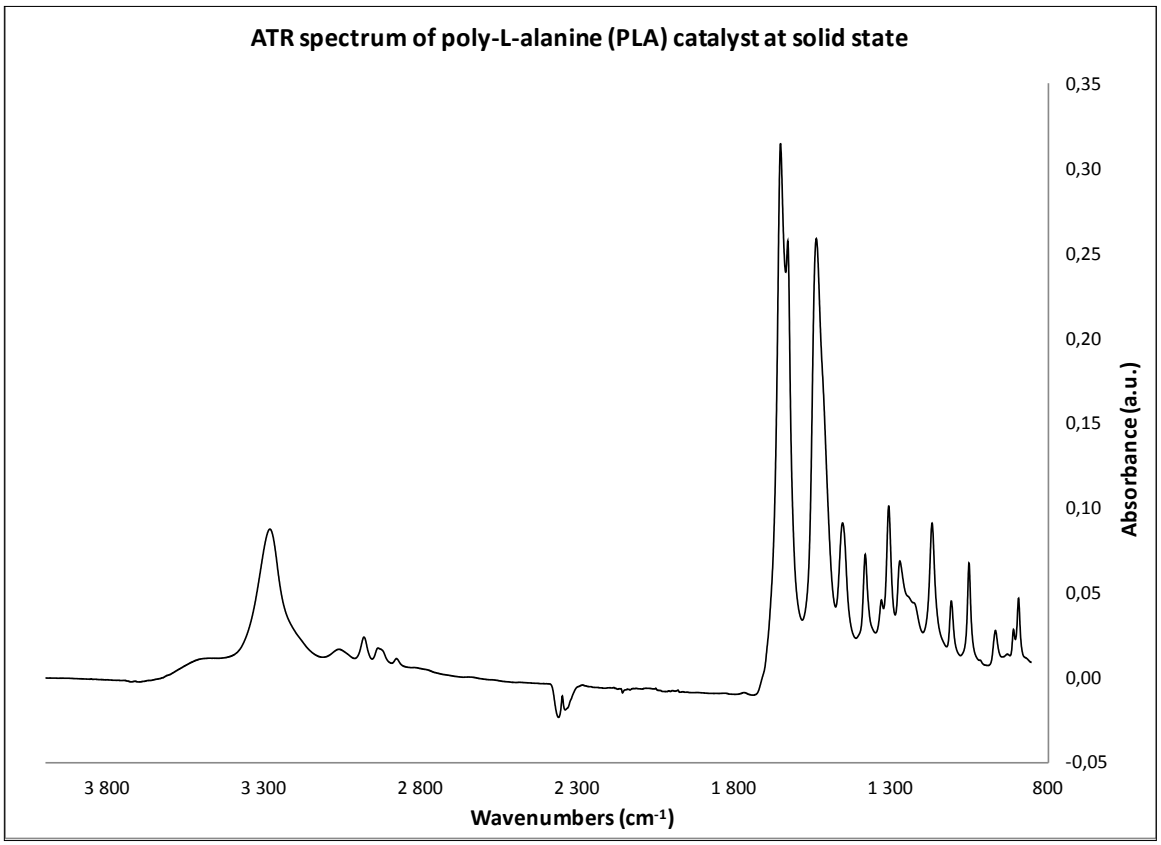
ATR spectrum of poly-L-alanine (PLA) catalyst at solid state
0,35
0,30
0,25
0,20
0,15
0,10
0,05
0,00
-0,05
Absorbance (a.u.)
3 800
3 300
2 800
2 300
1 800
1 300
800
Wavenumbers (cm-1)

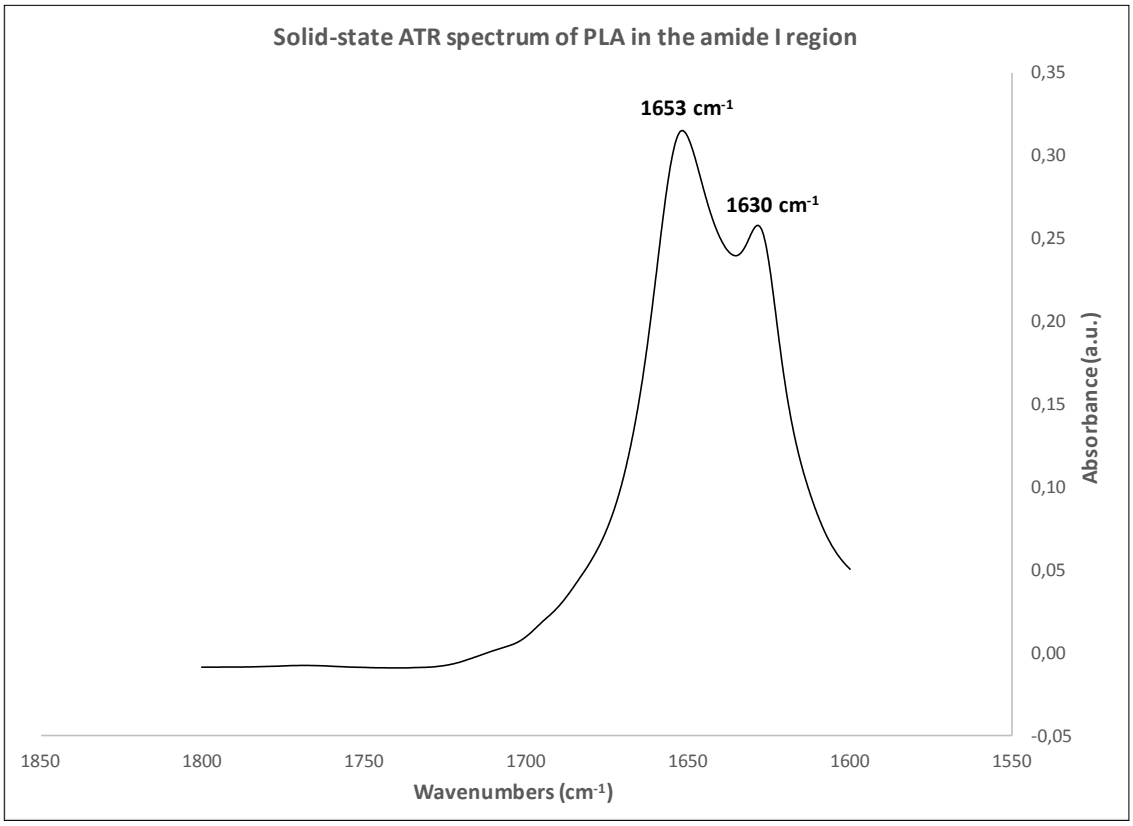
Solid-state ATR spectrum of PLA in the amide I region
1653 cm-1
1630 cm-1
0,35
0,30
0,25
0,20
0,15
0,10
0,05
0,00
-0,05
Absorbance (a.u.)
1850
1800
1750
1700
1650
1600
1550
Wavenumbers (cm-1)

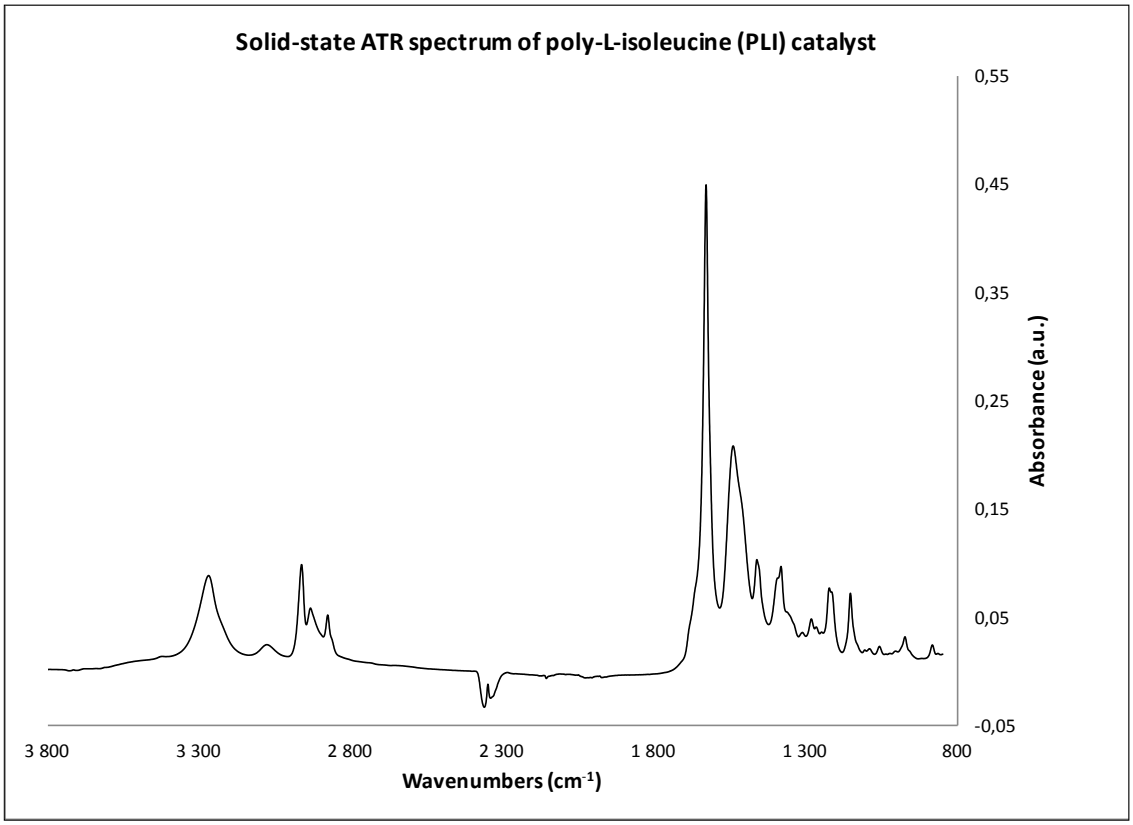
Solid-state ATR spectrum of poly-L-isoleucine (PLI) catalyst
0,55
0,45
0,35
0,25
0,15
0,05
-0,05
Absorbance (a.u.)
3 800
3 300
2 800
2 300
1 800
1 300
800
Wavenumbers (cm-1)

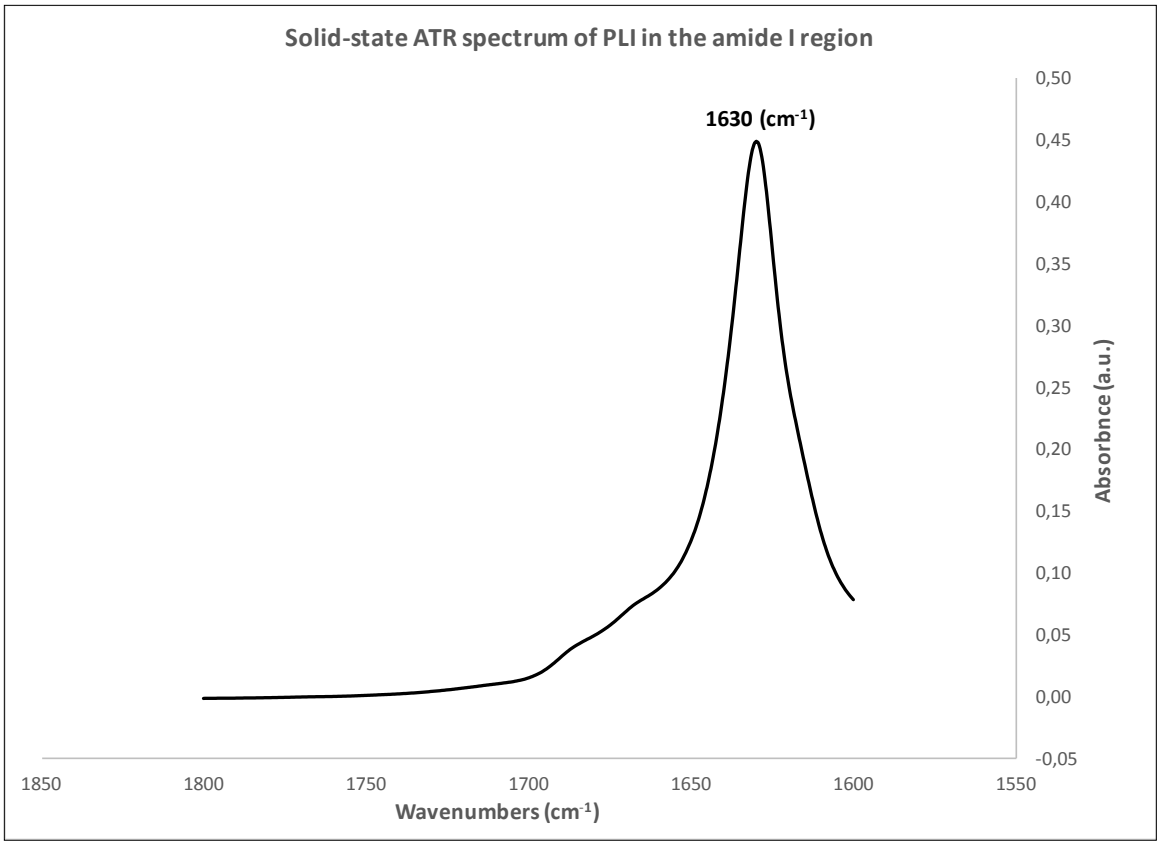
Solid-state ATR spectrum of PLI in the amide I region
1630 (cm-1)
0,50
0,45
0,40
0,35
0,30
0,25
0,20
0,15
0,10
0,05
0,00
-0,05
Absorbnce (a.u.)
1850
1800
1750
1700
1650
1600
1550
Wavenumbers (cm-1)

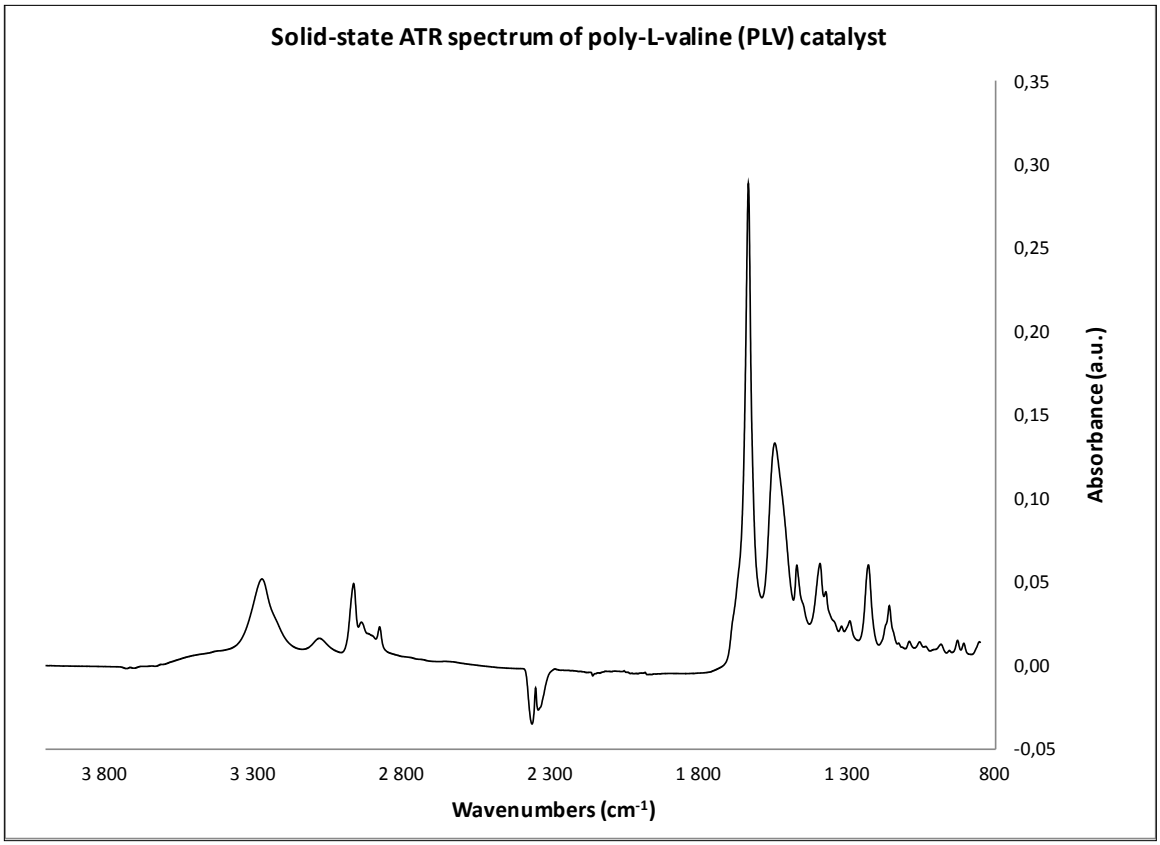
Solid-state ATR spectrum of poly-L-valine (PLV) catalyst
0,35
0,30
0,25
0,20
0,15
0,10
0,05
0,00
-0,05
Absorbance (a.u.)
3 800
3 300
2 800
2 300
1 800
1 300
800
Wavenumbers (cm-1)

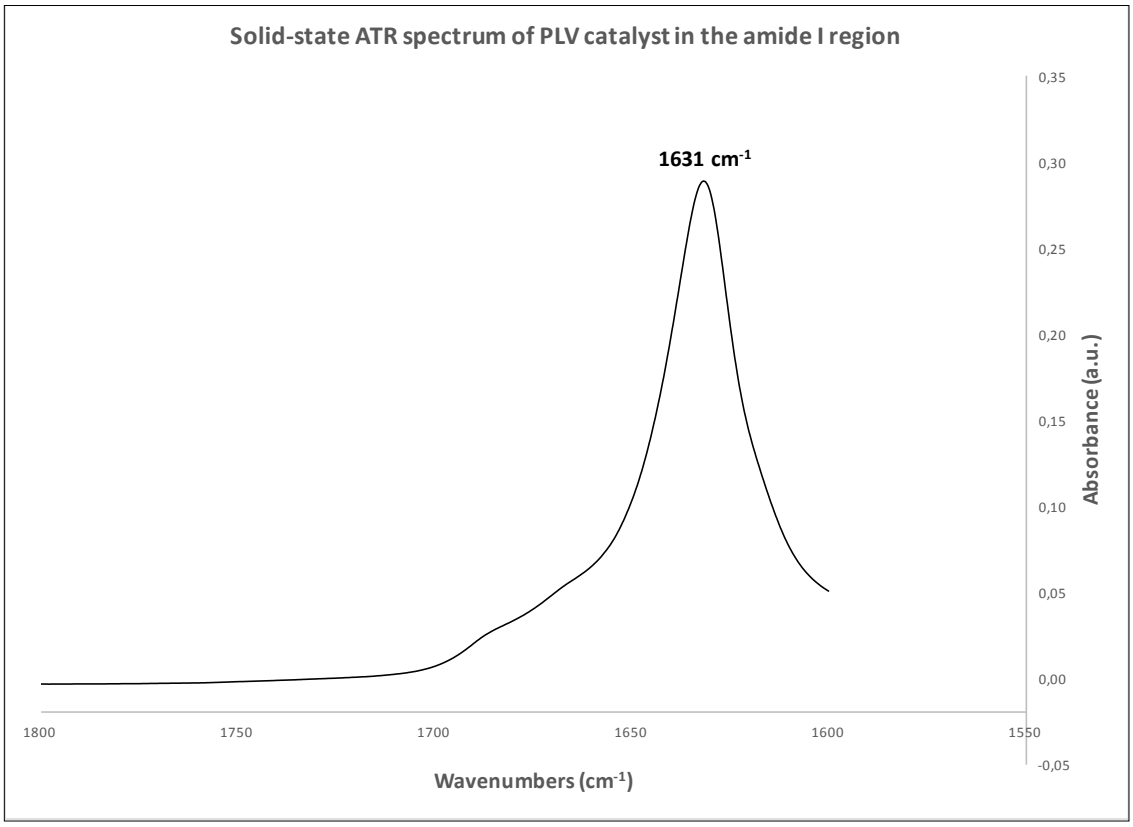
Solid-state ATR spectrum of PLV catalyst in the amide I region
1631 cm-1
0,35
0,30
0,25
0,20
0,15
0,10
0,05
0,00
-0,05
Absorbance (a.u.)
1800
1750
1700
1650
1600
1550
Wavenumbers (cm-1)

Solid-state ATR spectra of homo-oligopeptide catalysts in the amide I region

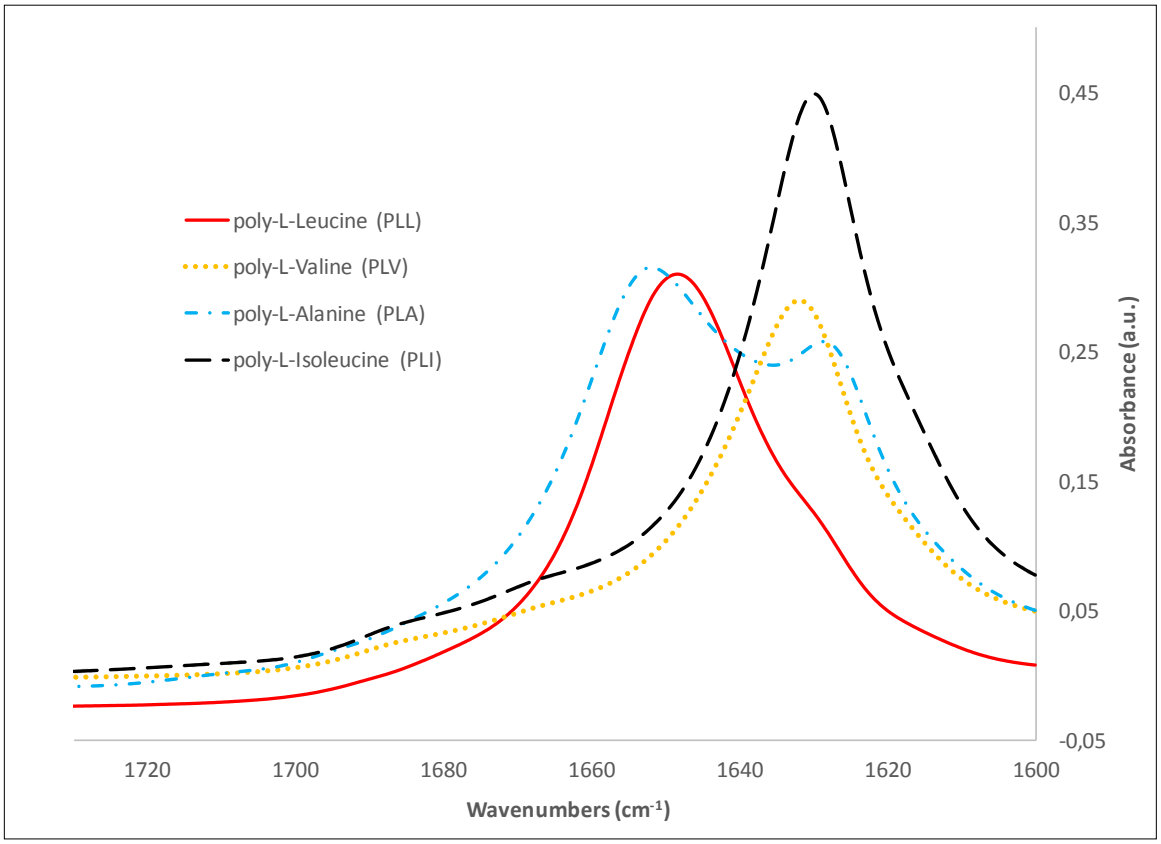

Previous mechanistic investigations suggested that oligopeptides that adopt a strong α-helical conformation are more efficient in this reaction than those that form β-sheets.[5] Consequently, we investigated the conformation of the oligomers in the solid state by ATR-FTIR using the amide I band, related to the peptide's secondary structure.[6] Results are shown in Figure 1. Interestingly, the intensity of the amide I band at 1655 cm^{-1} associated with the α-helical structure correlates with the epoxidation results obtained. For PLL and PLA, the amide I region of the IR spectra show strong bands at 1649 and 1653 cm^{-1} respectively. These observations suggest that PLL and PLA adopt mostly an α-helical conformation in water. However, in the cases of PLI and PLV that lead to racemic epoxide-**2a**, a strong absorption at 1630 cm^{-1} is observed and assigned to β-sheet structures. When performing the Julià-Colonna reaction in pure water, the propensity of the homo-oligopeptides for adopting an α-helical structure fits with epoxidation results, as in the triphasic system.

General procedure for the epoxidation of enones 2a-2k with PLL:

In a standard procedure, to a solution of the commercial PLL (0.005. mmol, 0.10 equiv.) in 1 mL of 50 mM Tris buffer pH 8 solution, enone (0.05 mmol, 1.0 equiv.) was added and stirred at room temperature for 1 h. Then, 50 *u*L of hydrogen peroxide (30%) was added after each 48 h period and the mixture was stirred with high at room temperature for one week. To ensure a good homogeneity of the mixture, the vessel was shaken frequently. Then, the corresponding epoxide was extracted with 0.3 mL of Et_2O. 20μL of the organic phase was added to a mixture of 1 : 1 AcOEt/H_2O. The organic phase was extracted and filtered with a 0.45 um PTFE filter and the conversion and the enantiomeric excess of the corresponding epoxides were determined by chiral HPLC using a Hewlett Packard series 1050 instrument.

Please note that the molecular weight of PLL used have been calculated based on the average of polymerisation degree.

Determination of enantiomeric excess for epoxy ketones

HPLC analysis

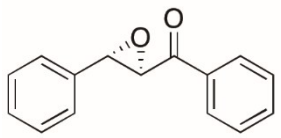

trans-(*2R,3S*)-Epoxy-1,3-diphenylpropan-1-one (***2a***).[7] HPLC (Chiralcel OD-H): λ 254 nm, hexanes/*i*-PrOH 95/5, flow rate 0.6 mL/min, $t_{R\ minor}$ (*2S,3R*) = 18.95 min, $t_{R\ major}$ (*2R,3S*) = 20.56 min.

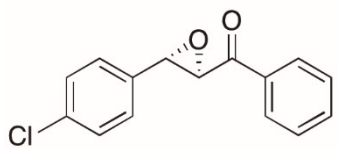

trans-(*2R,3S*)-Epoxy-3-(4-chlorophenyl)-1-phenyl-1-propan-1-one (***2b***).[7b,8] HPLC (Chiralcel OD-H): λ 254 nm, hexanes/*i*-PrOH 95/5, flow rate 0.6 mL/min, $t_{R\ minor}$ (*2S,3R*) = 20.53 min, $t_{R\ major}$ (*2R,3S*) = 21.87 min.

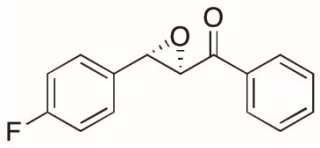

trans-(*2R,3S*)-Epoxy-3-(4-fluorophenyl)-1-phenyl-1-propan-1-one (***2c***).[7b,9] HPLC (Chiralcel AD-H): λ 254 nm, hexanes/*i*-PrOH 95/5, flow rate 0.6 mL/min, $t_{R\ minor}$ (*2S,3R*) = 28.71 min, $t_{R\ major}$ (*2R,3S*) = 31.29 min.

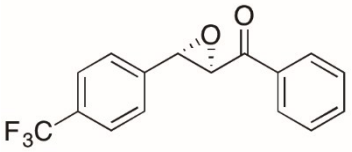

trans-(*2R,3S*)-Epoxy-3-(4-trifluorophenyl)-1-phenyl-1-propan-1-one (***2d***).[2] HPLC (Chiralcel OJ-H): λ 254 nm, hexanes/*i*-PrOH 95/5, flow rate 0.6 mL/min, $t_{R\ minor}$ (*2S,3R*) = 11.59 min, $t_{R\ major}$ (*2R,3S*) = 15.79 min.

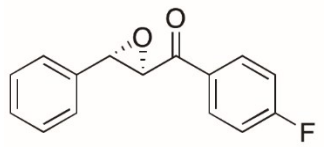

trans-(*2R,3S*)-2,3-epoxy-3-phenyl-1-(4-fluorophenyl)propan-1-one (***2e***).[7b,10] HPLC (Chiralcel OD-H): λ 254 nm, hexanes/*i*-PrOH 95/5, flow rate 0.6 mL/min, $t_{R\ minor}$ (*2S,3R*) = 21.22 min, $t_{R\ major}$ (*2R,3S*) = 22.86 min.

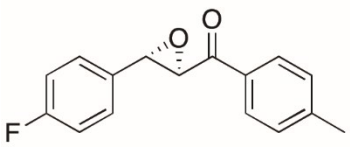

trans-(*2R,3S*)-2,3-epoxy-1-(4-methylphenyl)-3-(4-fluorophenyl)propan-1-one (***2f***).[7b,11] HPLC (Chiralcel AD-H): λ 254 nm, hexanes/*i*-PrOH 95/5, flow rate 0.6 mL/min, $t_{R\ minor}$ (*2S,3R*) = 36.92 min, $t_{R\ major}$ (*2R,3S*) = 44.01 min.

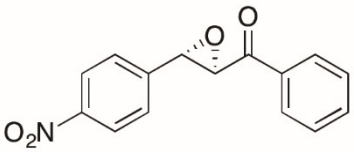

trans-(*2R,3S*)-Epoxy-3-(4-nitrophenyl)-1-phenyl-1-propan-1-one (***2g***).[7] HPLC (Chiralcel OD-H): λ 254 nm, hexanes/*i*-PrOH 95/5, flow rate 0.6 mL/min, $t_{R\ minor}$ (*2S,3R*) = 75.52 min, $t_{R\ major}$ (*2R,3S*) = 81.31 min.

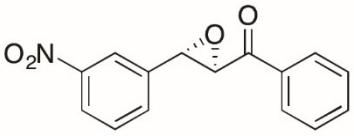

trans-(*2R,3S*)-Epoxy-3-(3-nitrophenyl)-1-phenyl-1-propan-1-one (***2h***).[7b] HPLC (Chiralcel OD-H): λ 254 nm, hexanes/*i*-PrOH 95/5, flow rate 0.6 mL/min, $t_{R\ minor}$ (*2S,3R*) = 57.78 min, $t_{R\ major}$ (*2R,3S*) = 64.17 min.

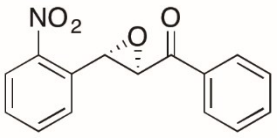

trans-(*2R,3S*)-Epoxy-3-(2-nitrophenyl)-1-phenyl-1-propan-1-one (***2i***).[7b] HPLC (Chiralcel OD-H): λ 254 nm, hexanes/*i*-PrOH 95/5, flow rate 0.6 mL/min, $t_{R\ major}$ (*2S,3R*) = 43.81 min, $t_{R\ minor}$ (*2R,3S*) = 50.21 min.

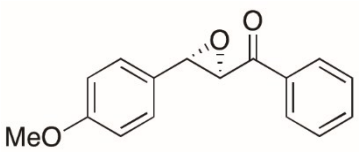

trans-(*2R,3S*)-Epoxy-3-(4-methoxyphenyl)-1-phenyl-1-propan-1-one (***2j***). [2] HPLC (Chiralcel AD-H): λ 254 nm, hexanes/*i*-PrOH 95/5, flow rate 0.6 mL/min, $t_{R\ minor}$ (*2S,3R*) = 24.14 min, $t_{R\ major}$ (*2R,3S*) = 29.43 min.

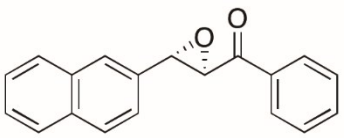

(*2R,3S*)-3-(naphthalen-2-yl)-1-phenylprop-2-en-1-one[2] (***2k***). HPLC (Chiralcel AD-H): λ 254 nm, hexanes/*i*-PrOH 95/5, flow rate 0.6 mL/min, $t_{R\ minor}$ (*2S,3R*) = 28.31 min, $t_{R\ major}$ (*2R,3S*) = 33.60 min.

The absolute configuration of epoxides **2a-2k** was determined by comparison of the HPLC retention times and elution order of the corresponding epoxides with literature values. In addition, the first signal on each chromatogram correspond to the starting enones.

*Please note that the epoxidation of each enone has been done twice and the average of both conversion and enantiomeric excess are reported. Typical chromatograms obtained for each epoxyketone are illustrated below.

Bench marking of homo-oligopeptides synthesized in the initial triphasic system[12]

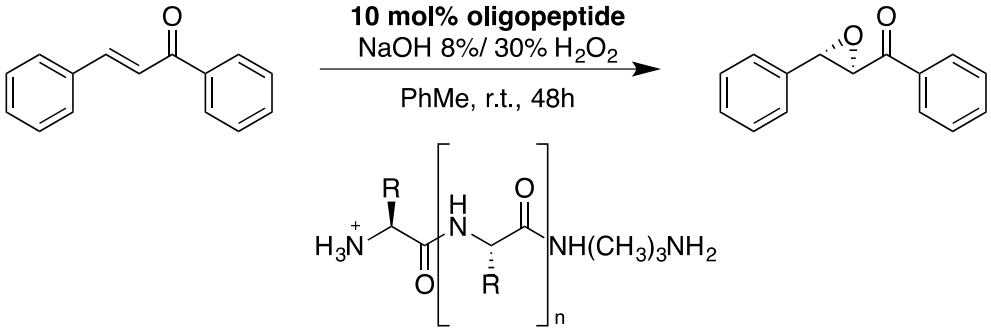

General procedure epoxidation of chalcones with homo-oligopeptide catalysts in a triphasic system

In a standard procedure, homo-oligopeptide (0.01 mmol, 0.10 equiv.) was added to a solution of chalcone **1** (0.1 mmol, 1.0 equiv.) in toluene for 30 min. Then, 0.20 mL of a solution of 8% NaOH in 30% hydrogen peroxide (0.08 g/mL) was added and the mixture was stirred at room temperature for 48 h. Then, the corresponding epoxide was extracted with 0.3 mL of Et_2O. 20 μL of the organic phase was added to a mixture of 1 : 1 AcOEt/H_2O. The organic phase was extracted and filtered with a 0.45 um PTFE filter and the conversion and the enantiomeric excess of the corresponding epoxides were determined by chiral HPLC using a Hewlett Packard series 1050 instrument.

Triphasic system epoxidation results of 1 using PLL

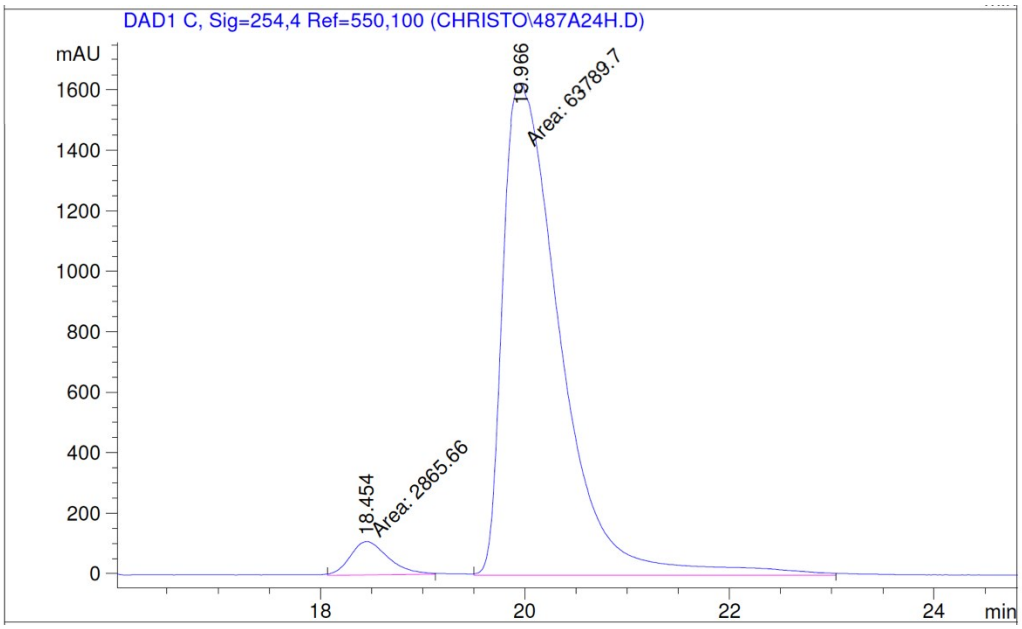

99% conversion, 96% (*2R,3S*)-epoxychalcone **2a**

Triphasic system epoxidation results of 1 using PLA

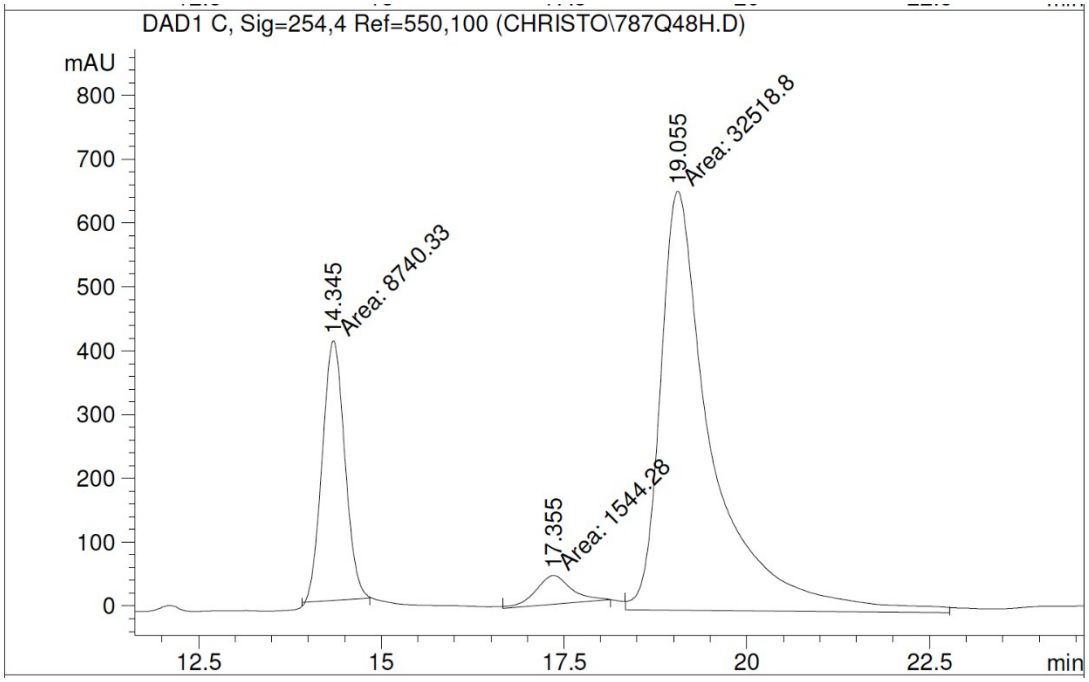

80% conversion, 91% (*2R,3S*)-epoxychalcone **2a**

Triphasic system epoxidation results of 1 using PLI

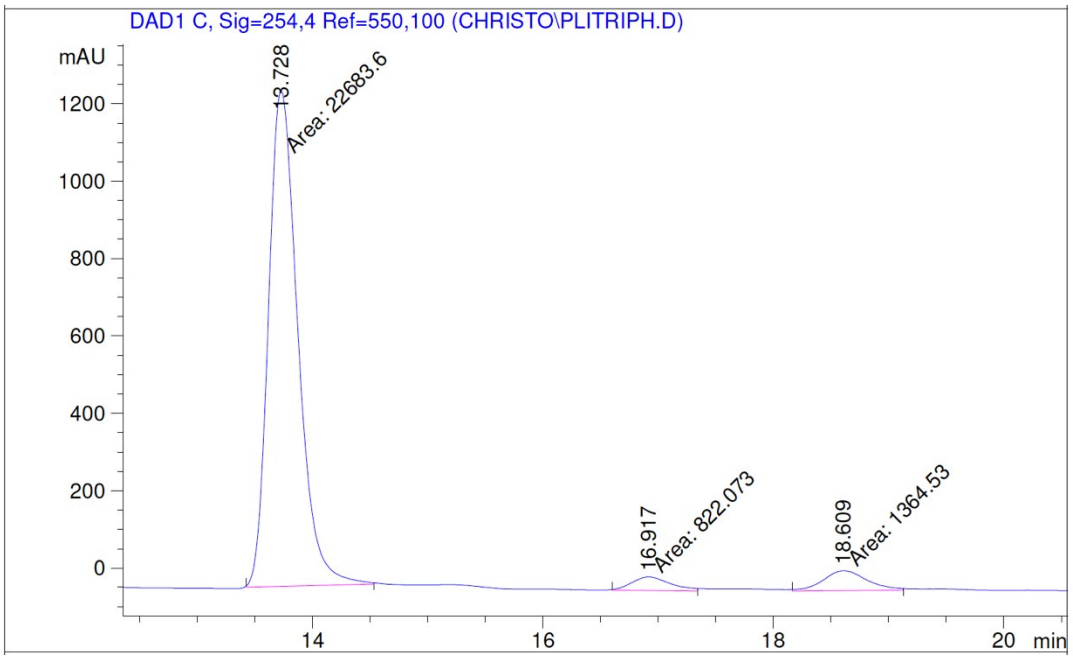

9% conversion, 25% (*2R,3S*)-epoxychalcone **2a**

Triphasic system epoxidation results of 1 using PLV

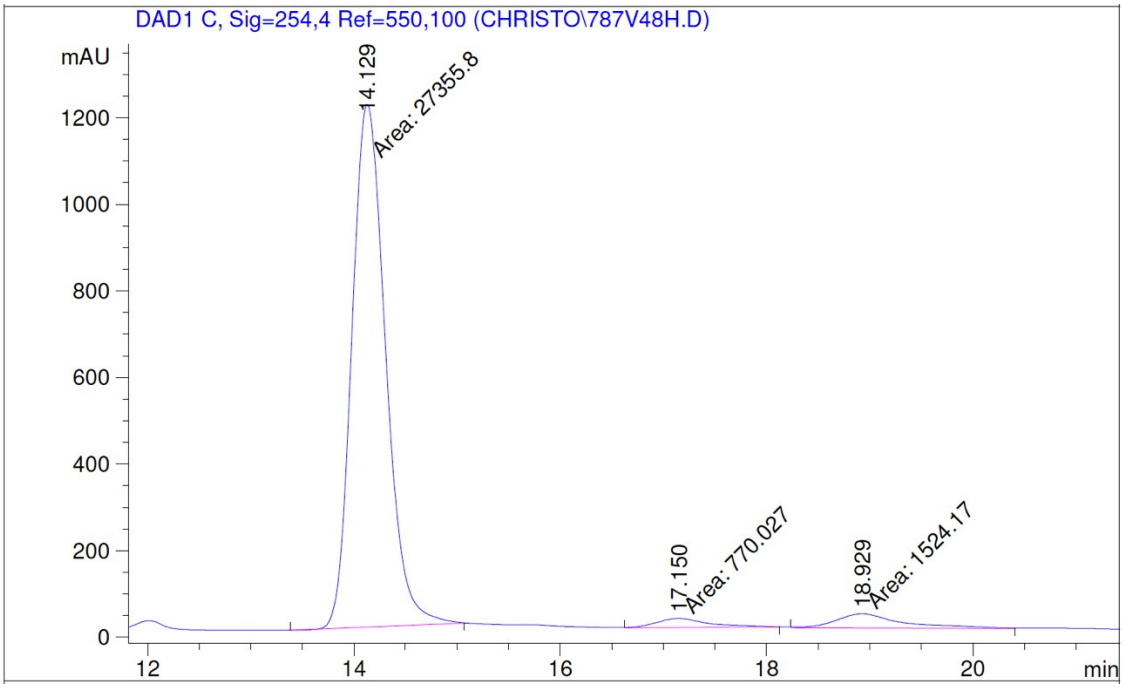

8% conversion, 32% (*2R,3S*)-epoxychalcone **2a**

Optimisation of buffer with PLL (1 mol%)

Table 1, entry 4 (pH = 8)

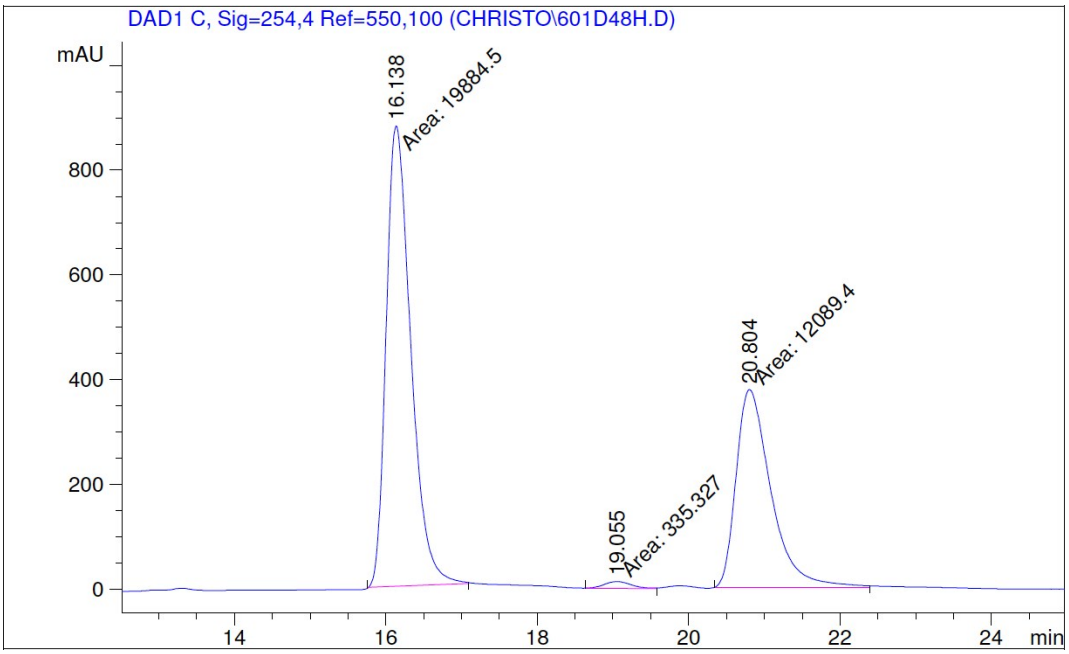

38% conversion, 95% (*2R,3S*)-epoxychalcone **2a**

Table 1, entry 5 (pH = 10)

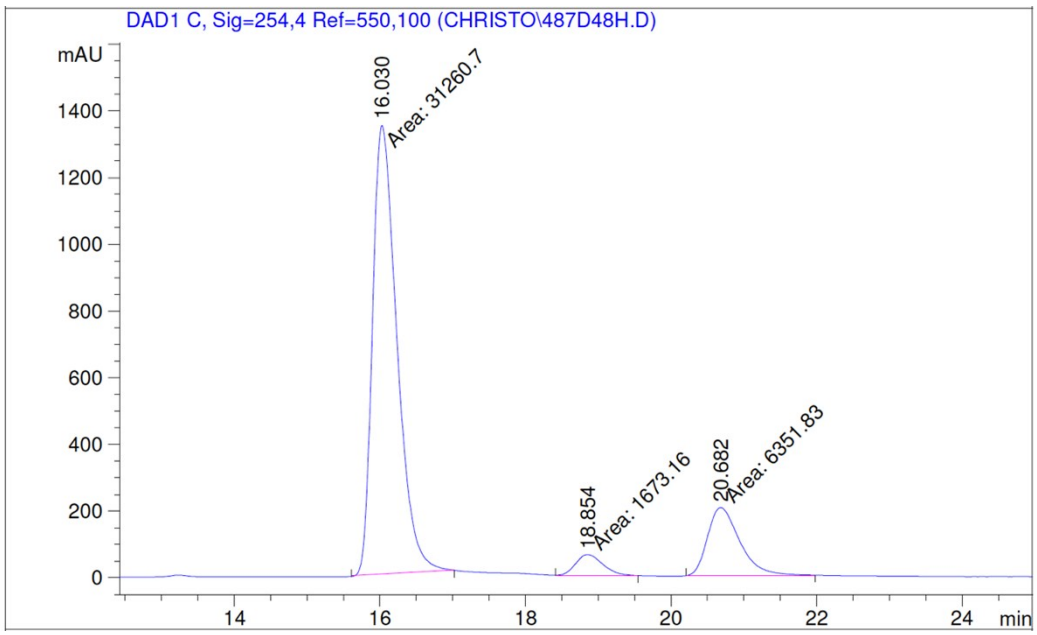

48% conversion, 80% (*2R,3S*)-epoxychalcone **2a**

Table 1, entry 6 (pH = 12)

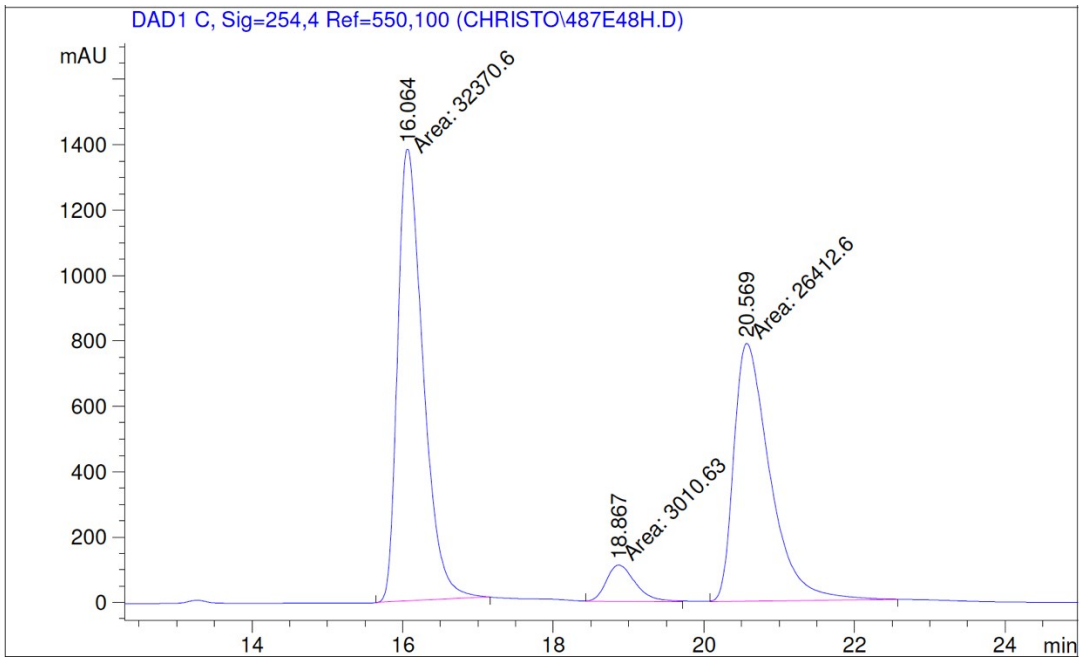

53% conversion, 75% (*2R,3S*)-epoxychalcone **2a**

Optimisation of PLL loading

Table 1, entry 4 (1 mol% PLL)

38% conversion, 95% (*2R,3S*)-epoxychalcone **2a**

Table 1, entry 7 (2.5 mol% PLL)

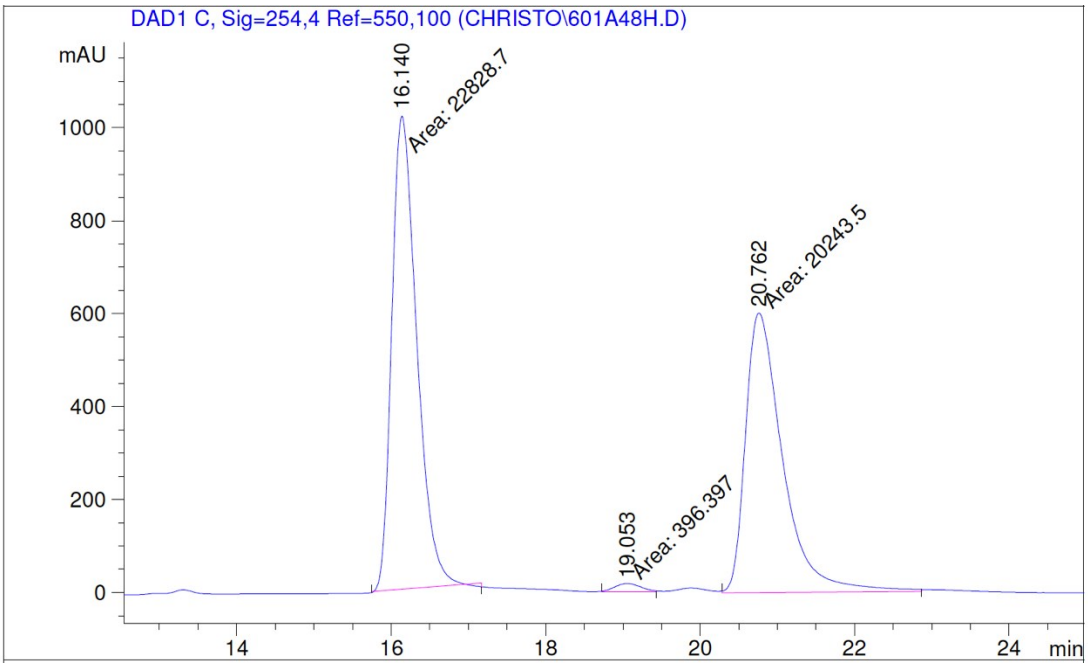

48% conversion, 96% (*2R,3S*)-epoxychalcone **2a**

Table 1, entry 8 (5 mol% PLL)

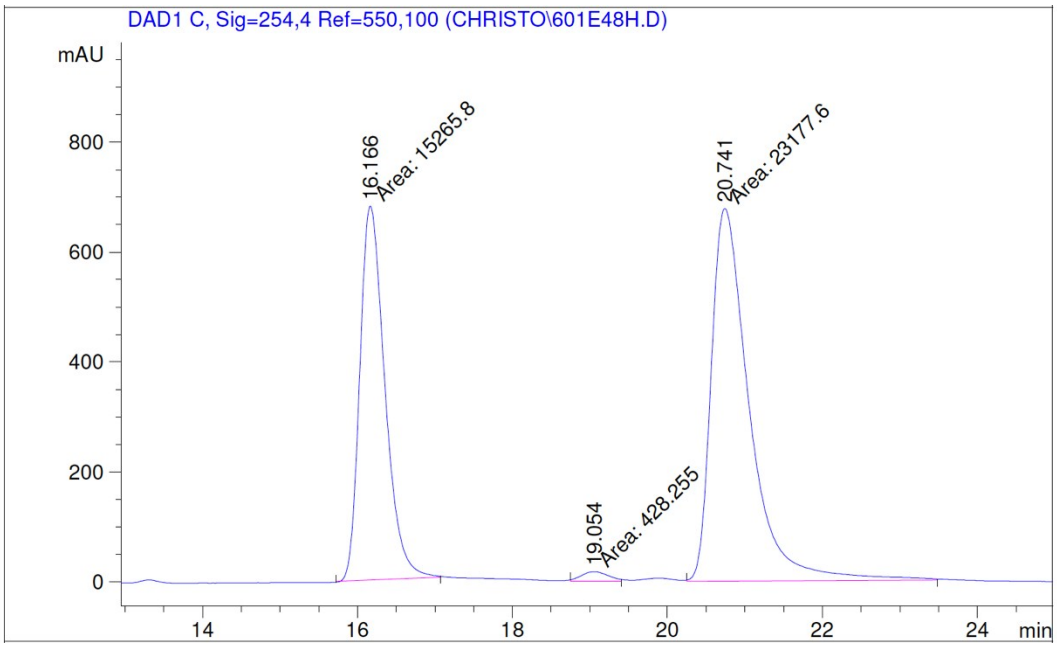

61% conversion, 96% (*2R,3S*)-epoxychalcone **2a**

Table 1, entry 9 (10 mol% PLL)

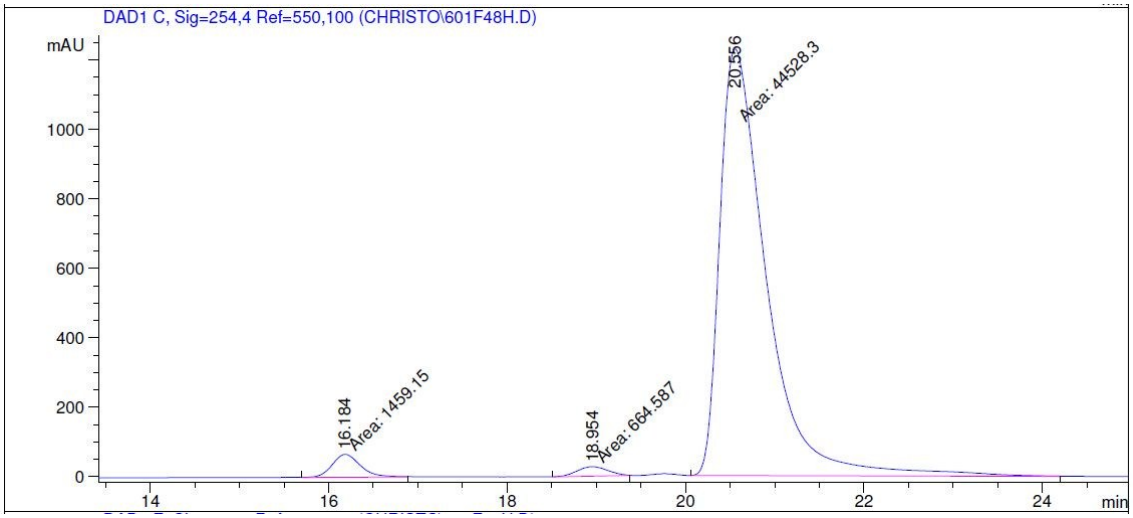

97% conversion, 97% (*2R,3S*)-epoxychalcone **2a**

Epoxydation in pure water using PLA

Table 1, entry 10

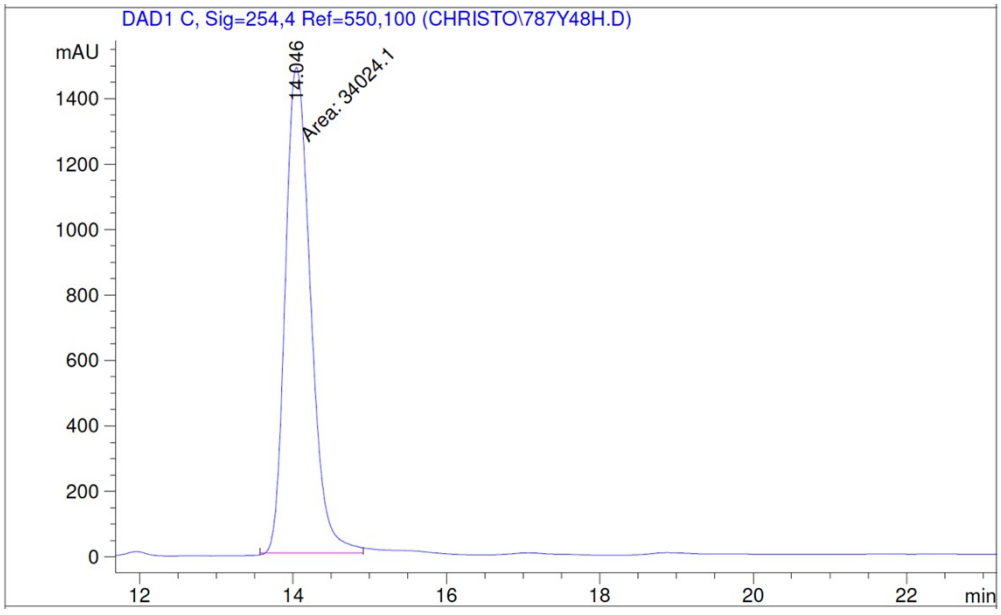

<5% conversion, 0% ee

Epoxydation in pure water using PLI

Table 1, entry 11

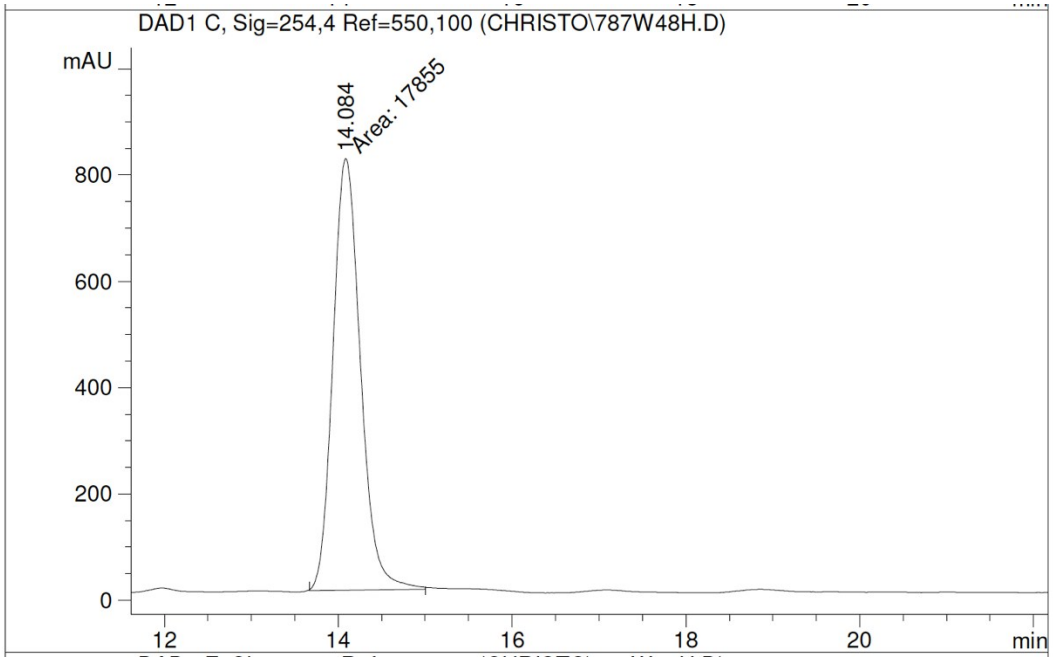

Epoxydation in pure water using PLV

Table 1, entry 12

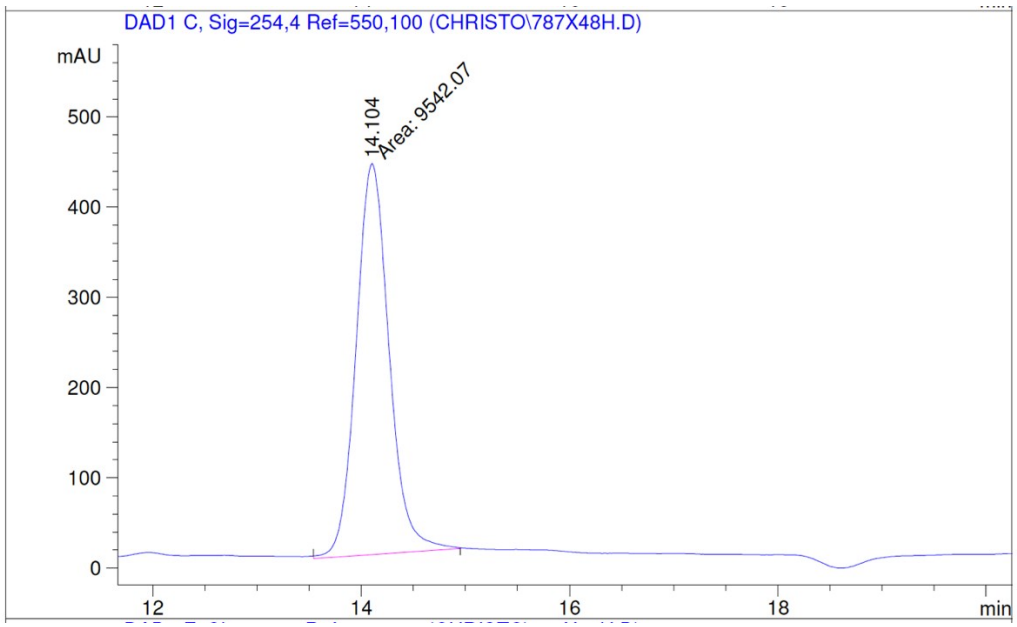

<5% conversion, 0% ee

Substrates scope

trans-(*2R,3S*)-Epoxy-1,3-diphenylpropan-1-one (***2a***).

trans-(*2R,3S*)-Epoxy-3-(4-chlorophenyl)-1-phenyl- 1-propan-1-one (***2b***).

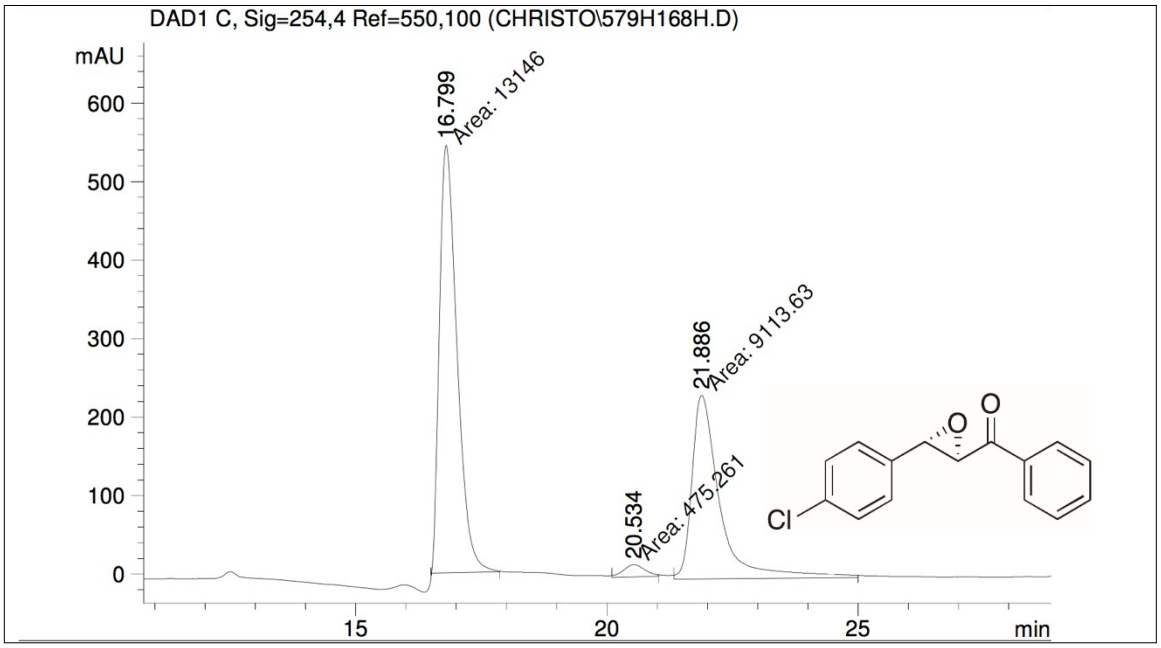

trans-(*2R,3S*)-Epoxy-3-(4-fluorophenyl)-1-phenyl- 1-propan-1-one (***2c***).

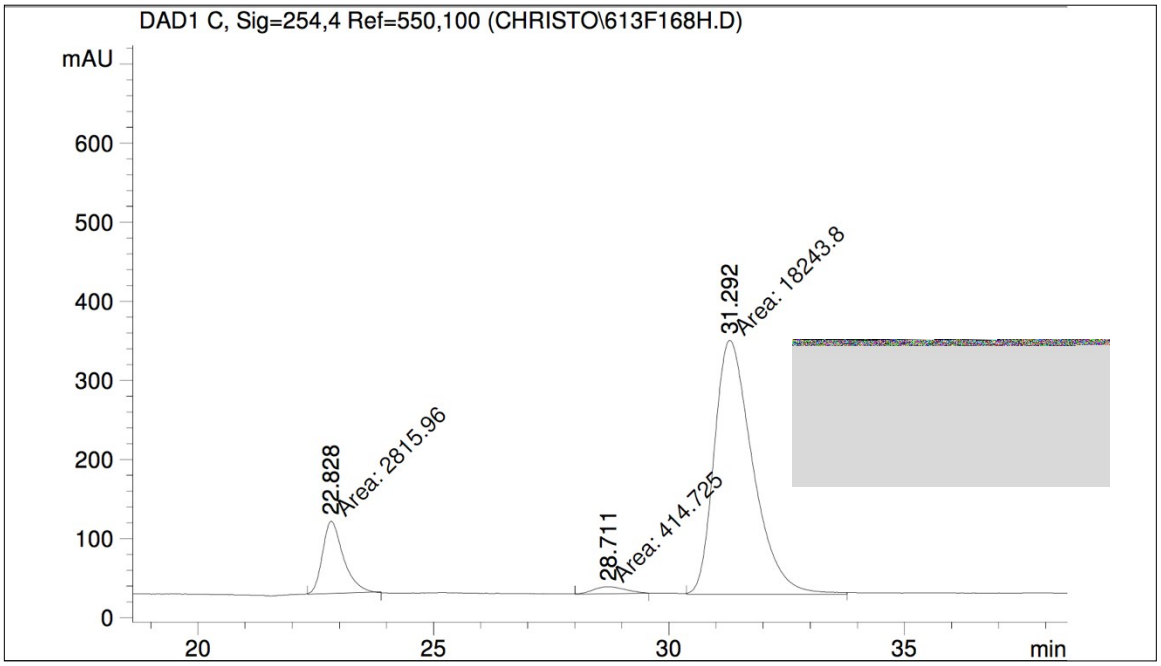

trans-(*2R,3S*)-Epoxy-3-(4-trifluorophenyl)-1-phenyl-1-propan-1-one ***(2d)***.

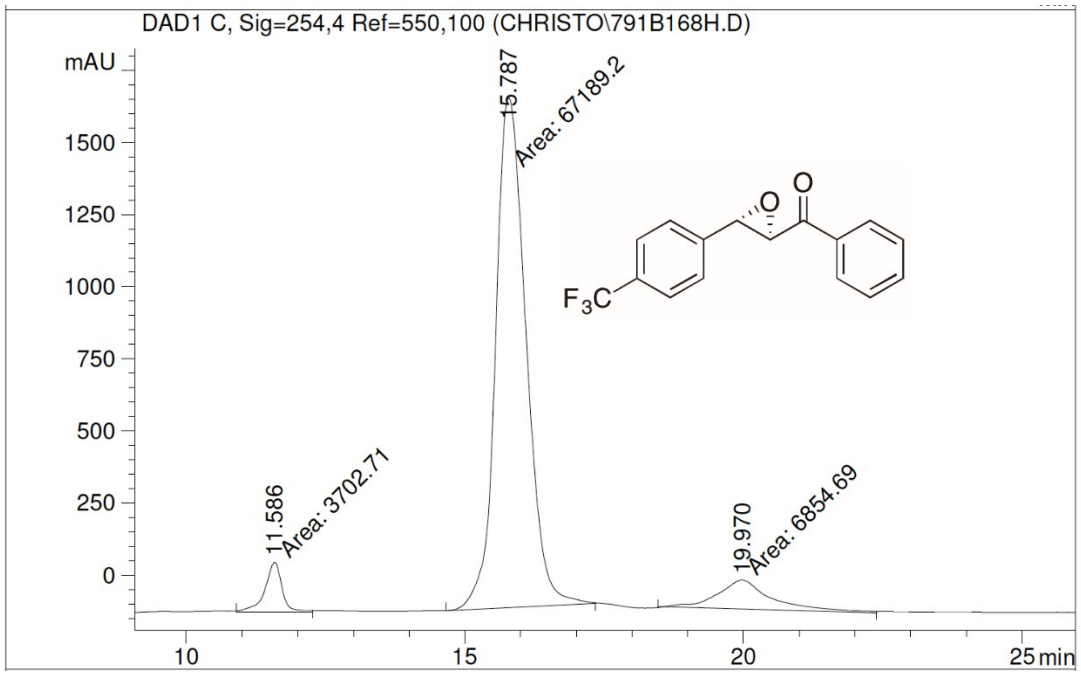

trans-(*2R,3S*)-2,3-epoxy-3-phenyl-1-(4-fluorophenyl)propan-1-one (***2e***).

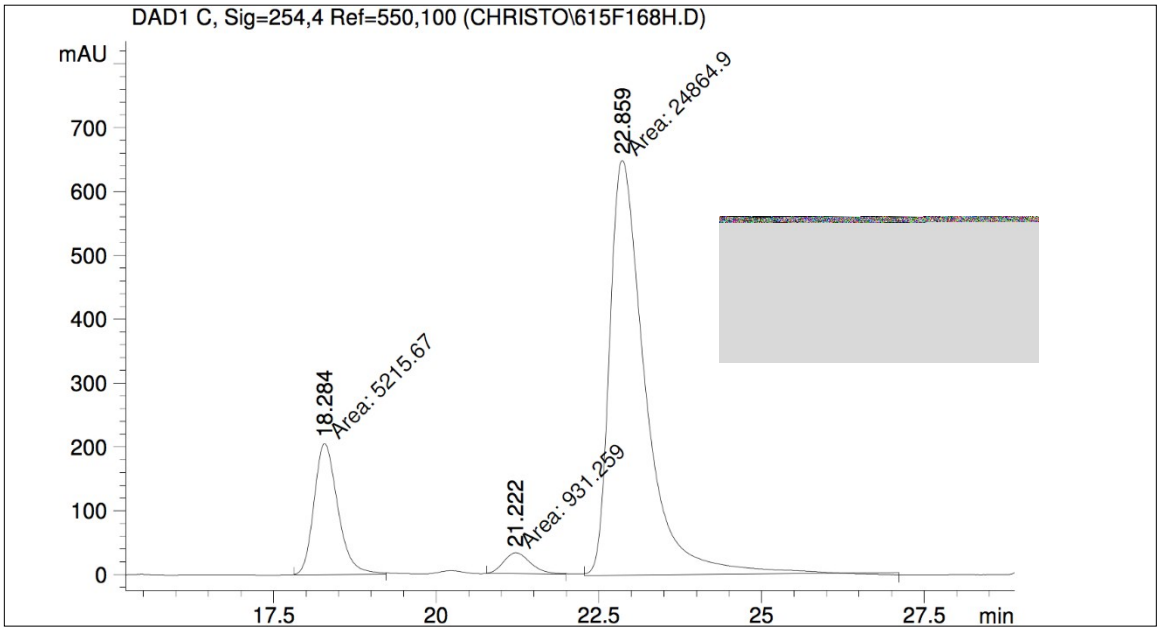

trans-(*2R,3S*)-2,3-epoxy-1-(4-methylphenyl)-3-(4-fluorophenyl)propan-1-one (***2f***).

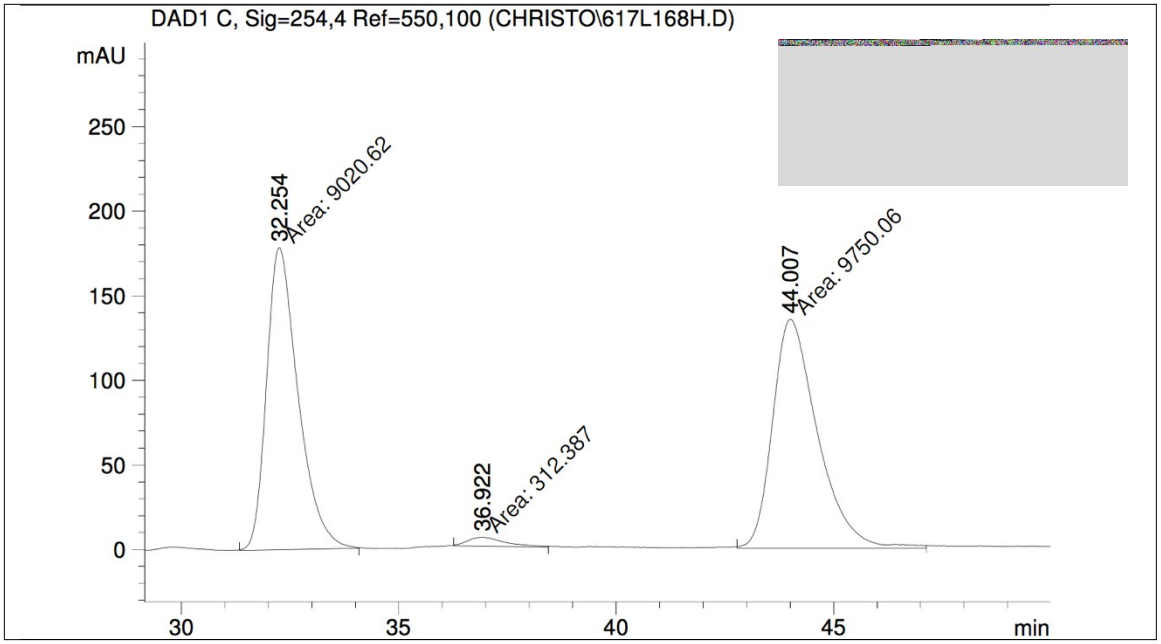

trans-(*2R,3S*)-Epoxy-3-(4-nitrophenyl)-1-phenyl- 1-propan-1-one (***2g***).

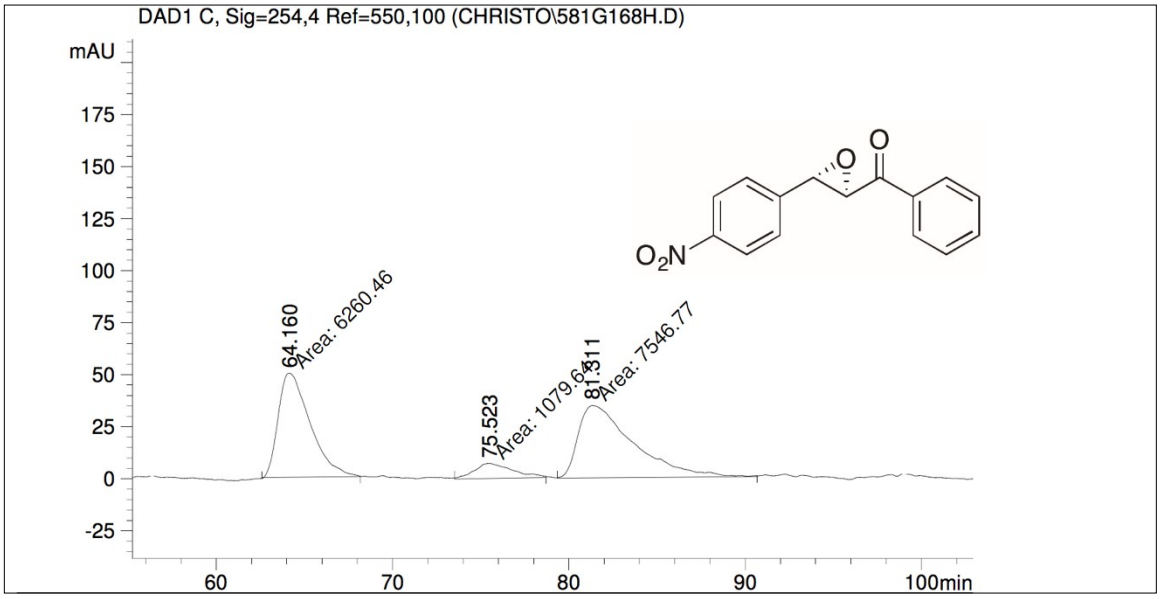

trans-(*2R,3S*)-Epoxy-3-(3-nitrophenyl)-1-phenyl- 1-propan-1-one (***2h***).

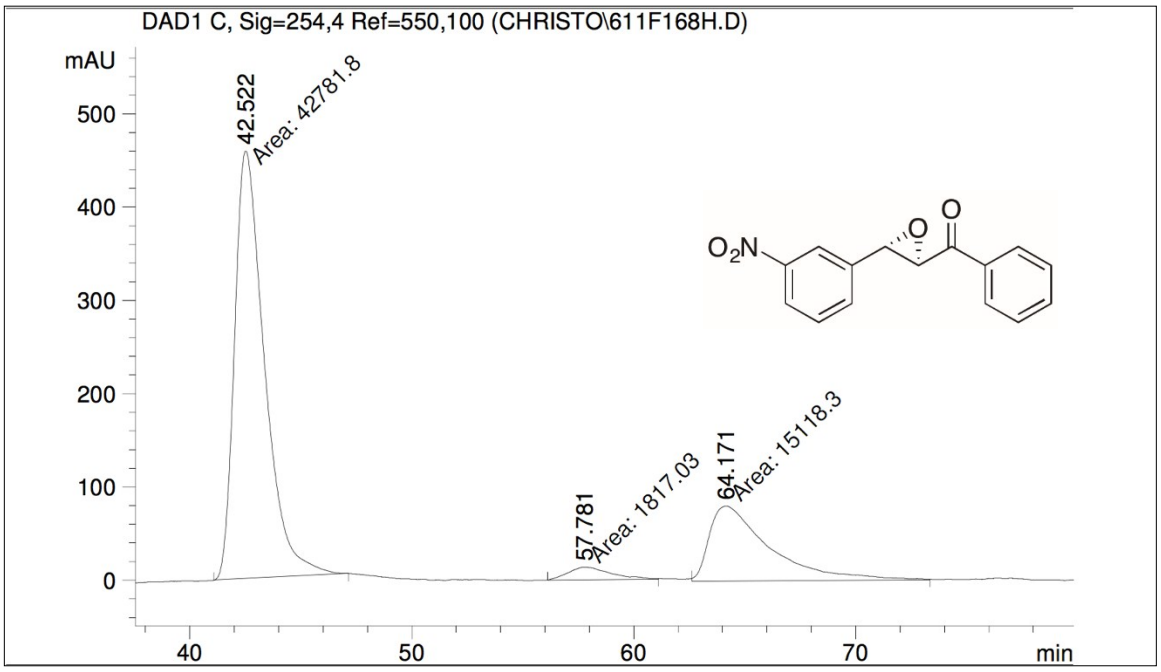

trans-(*2R,3S*)-Epoxy-3-(2-nitrophenyl)-1-phenyl- 1-propan-1-one (***2i***).

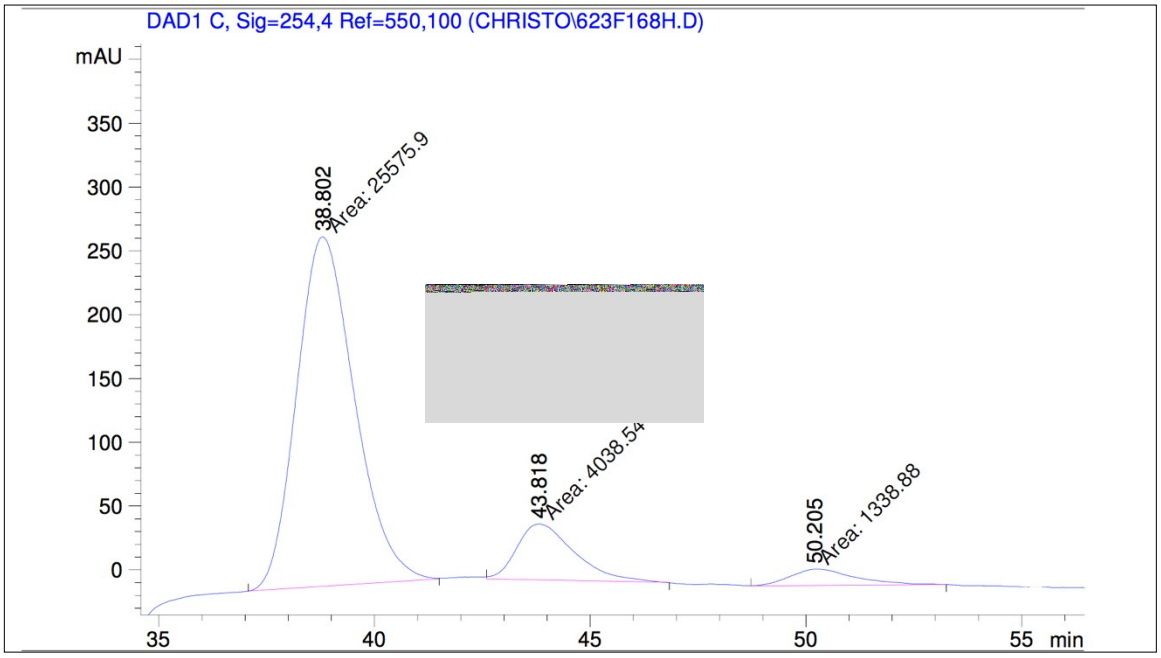

trans-(*2R,3S*)-Epoxy-3-(4-methoxyphenyl)-1-phenyl- 1-propan-1-one (***2j***).

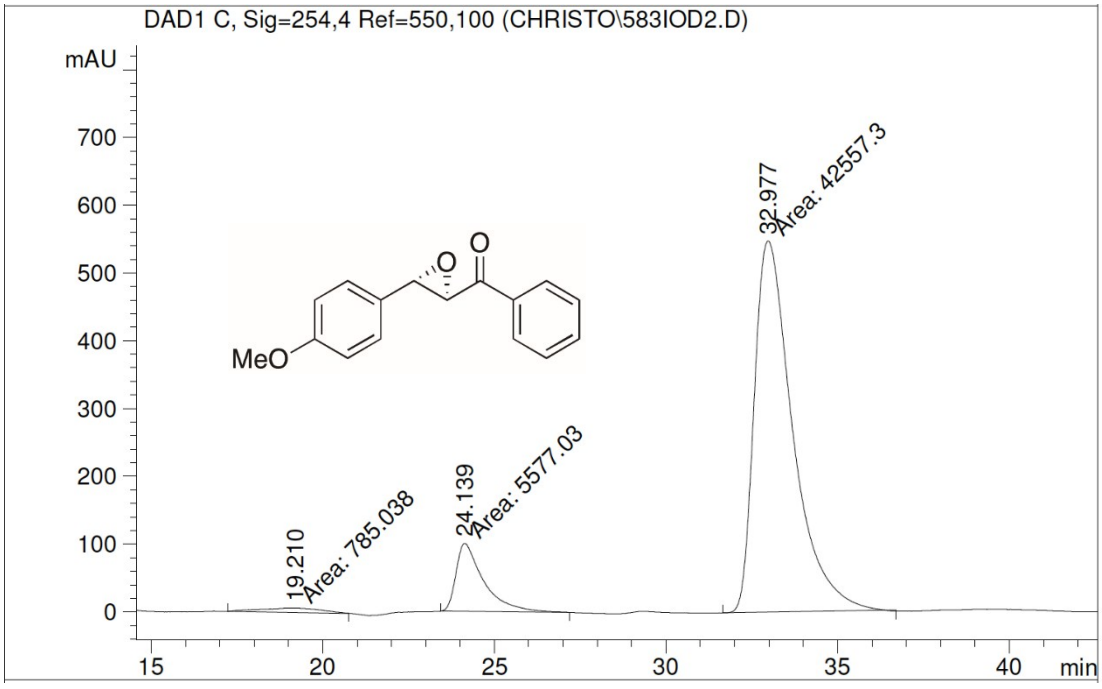

(*2R,3S*)-3-(naphthalen-2-yl)-1-phenylprop-2-en-1-one (***2k***).

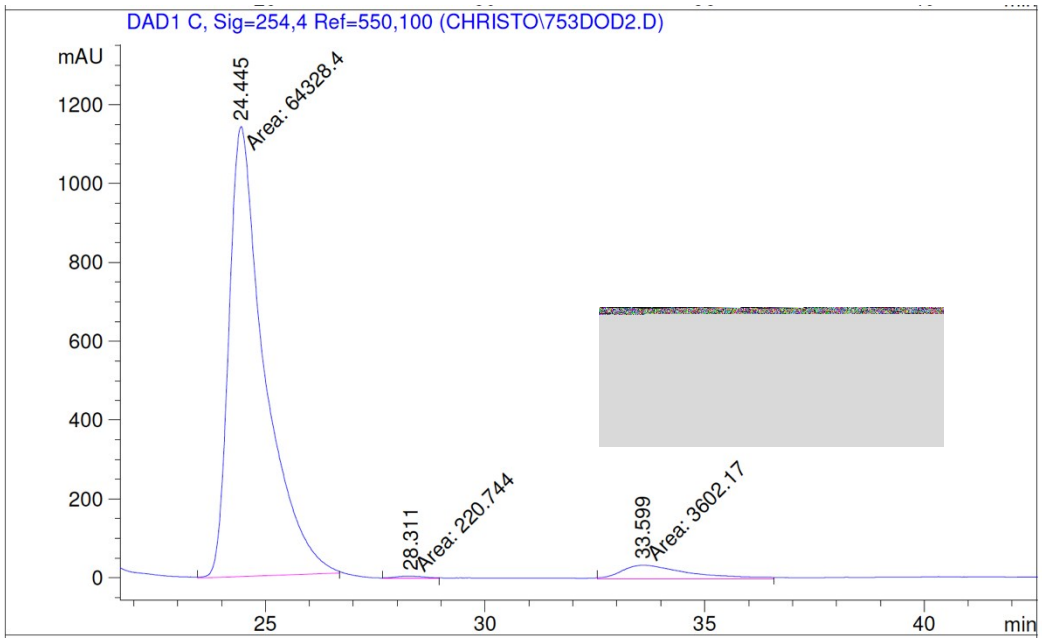

General procedure for PLL recovery and reuse:

After the epoxidation reaction with *trans*-chalcone **1**, PLL was recovered by filtration and the precipitate was washed with water and diethylether. Then, the recovered PLL was dried under vacuum and reused in the enantioselective epoxidation using the same protocol described above. Below, chromatograms of **2a** obtained with recovered PLL.

1st run (Initial reaction)

trans-(*2R,3S*)-Epoxy-1,3-diphenylpropan-1-one (***2a***).

97 % conversion, 97 % ee

2nd run

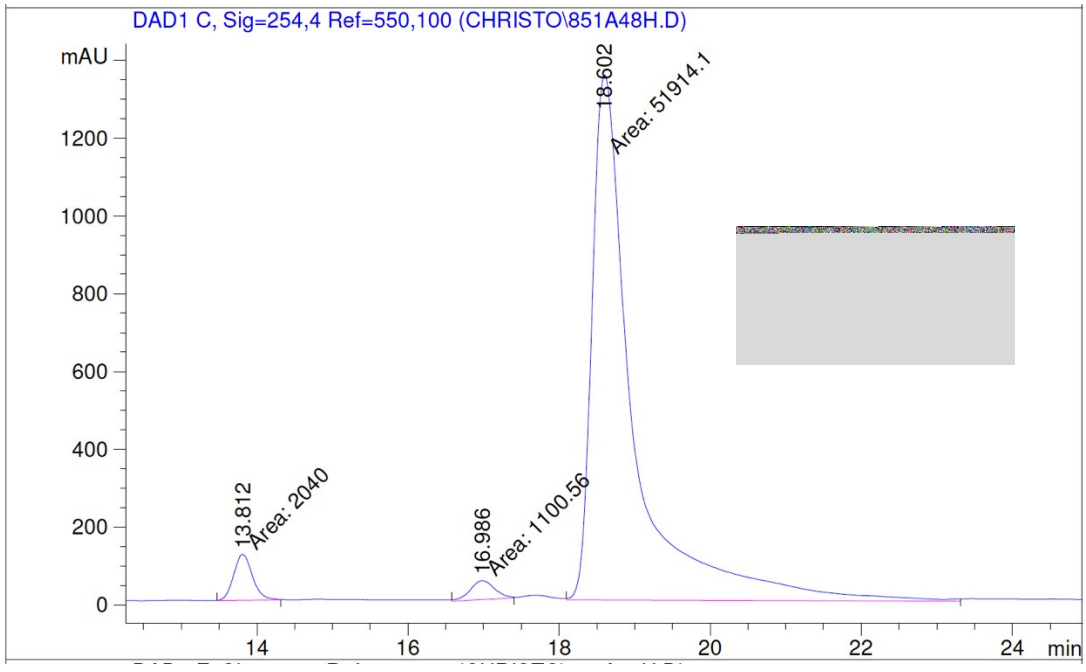

96% conversion, 96 % ee

3rd run

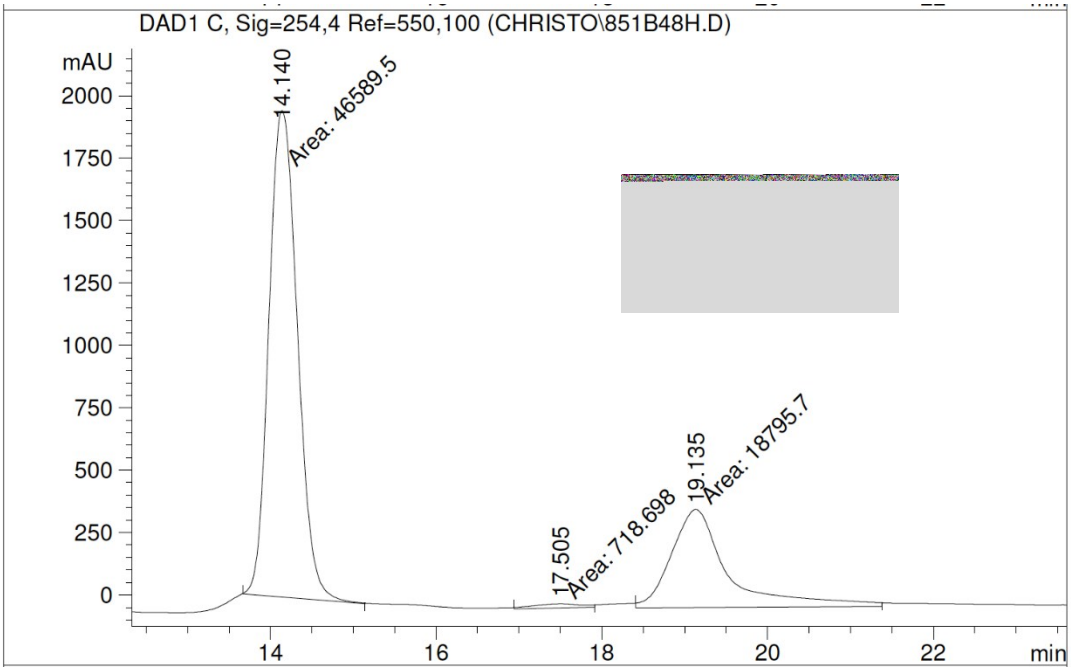

30 % conversion, 93 % ee

4rd run

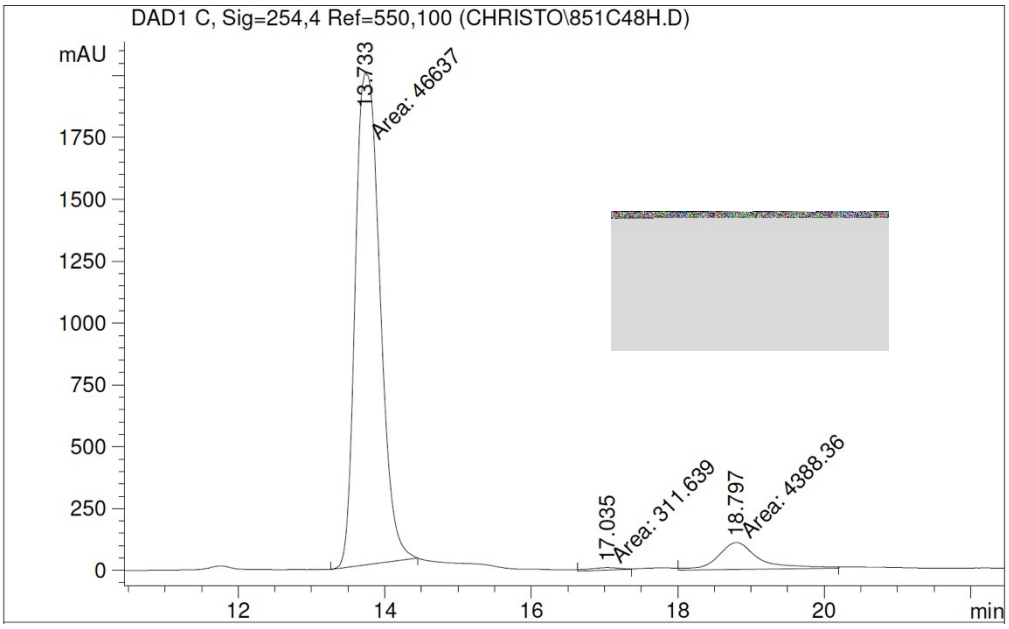

10 % conversion, 87 % ee

^{1}H-NMR spectrum of L-leucine *N*-Carboxyanhydride

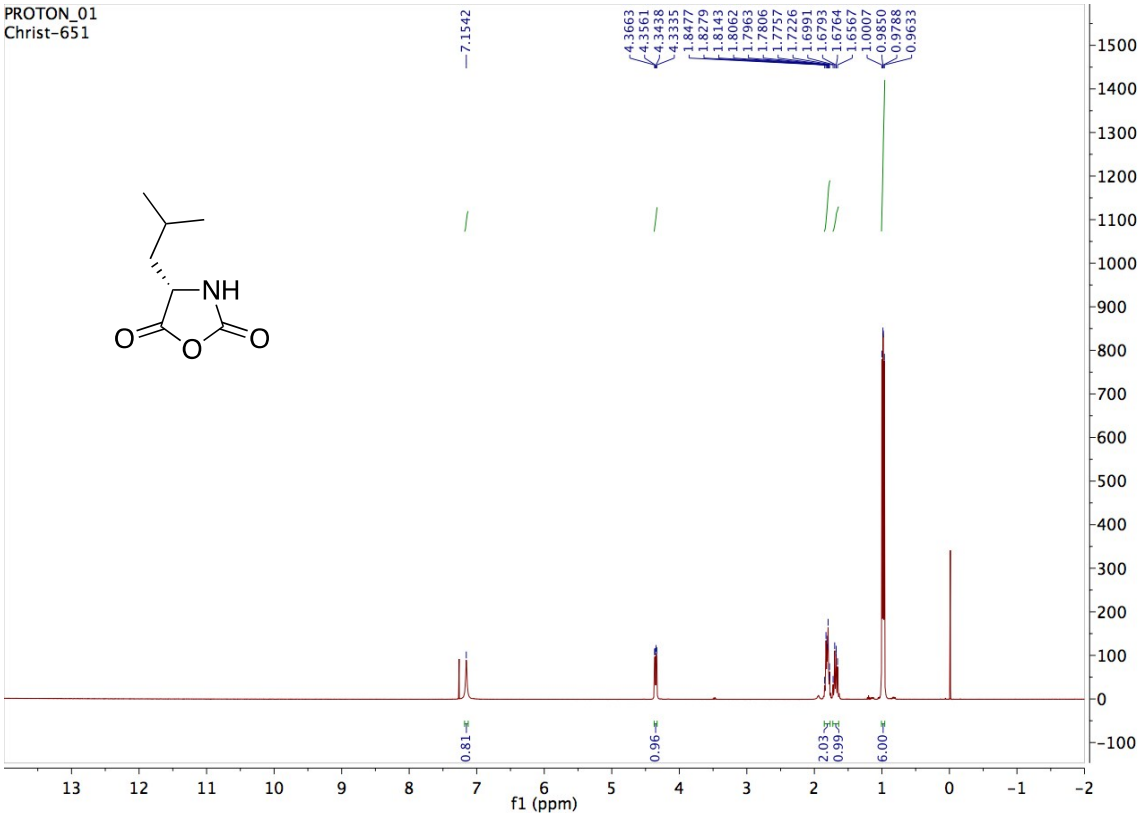

^{13}C-NMR spectrum of L-leucine *N*-Carboxyanhydride

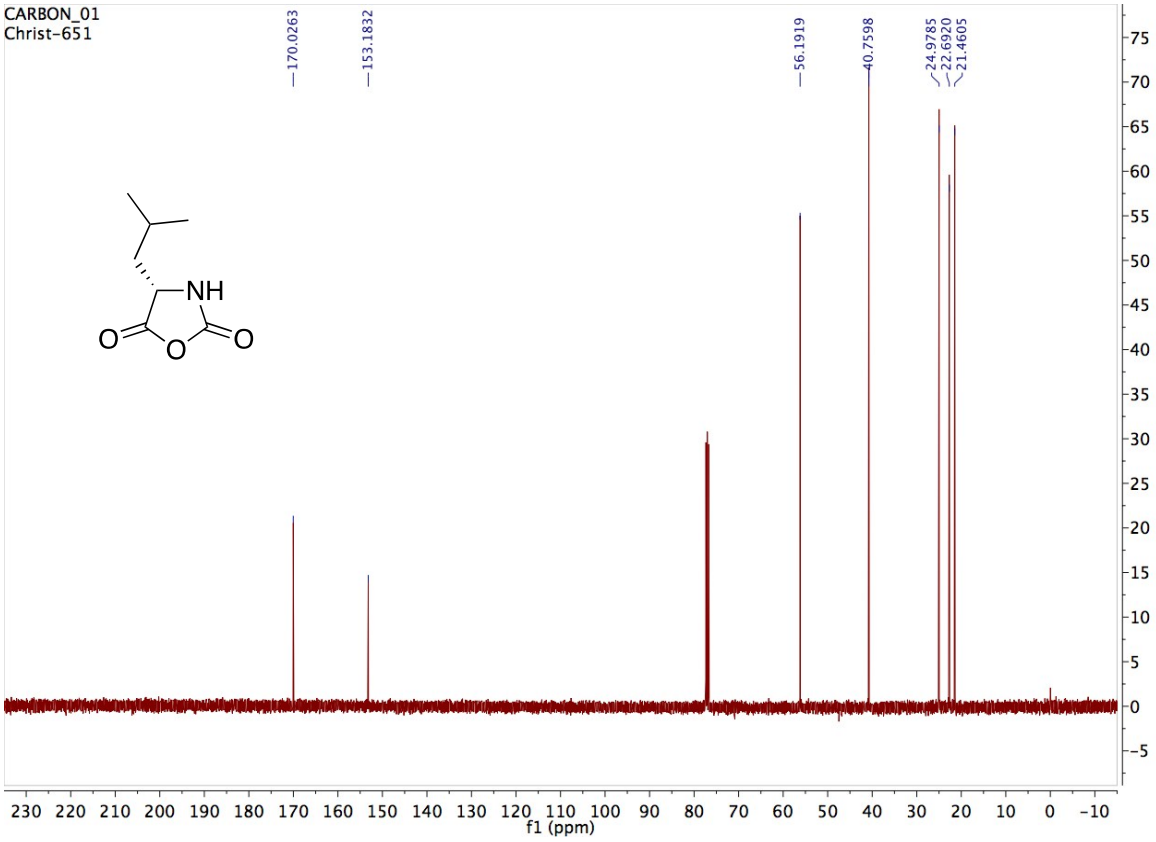

^{1}H-NMR spectrum of L-Isoleucine *N*-Carboxyanhydride

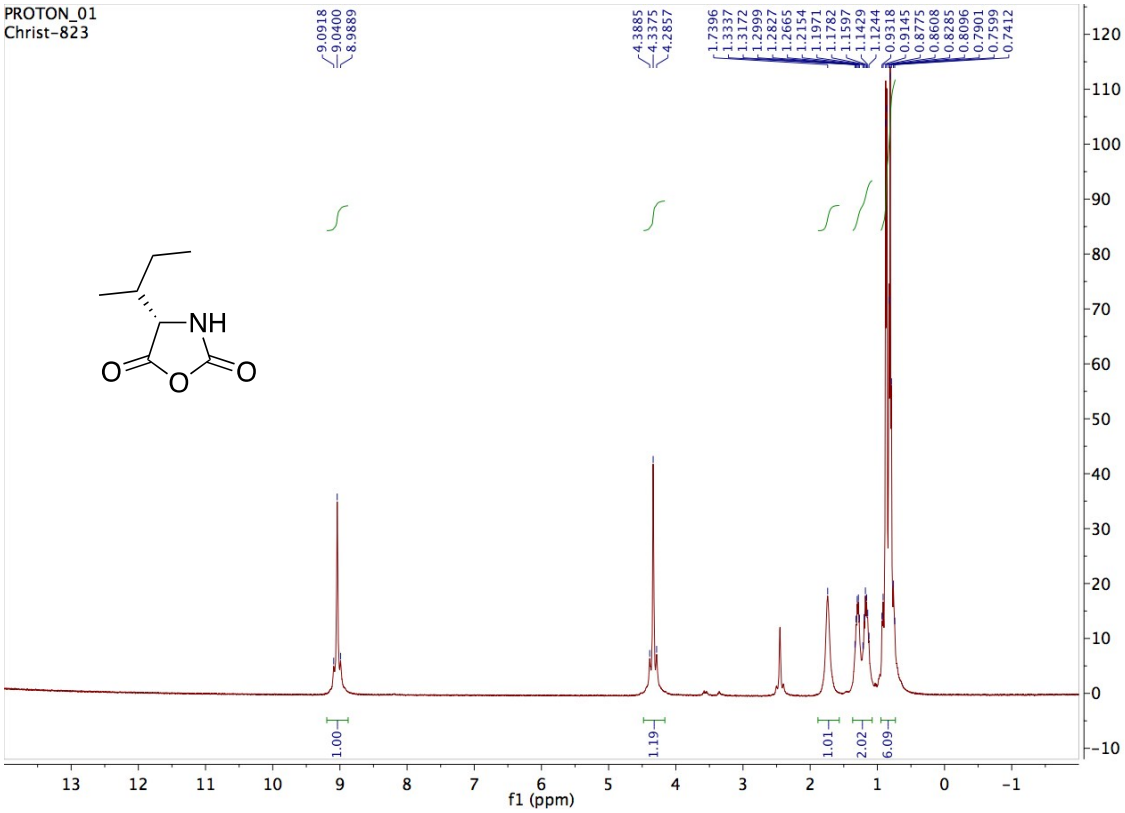

^{1}H-NMR spectrum of L-Isoleucine *N*-Carboxyanhydride

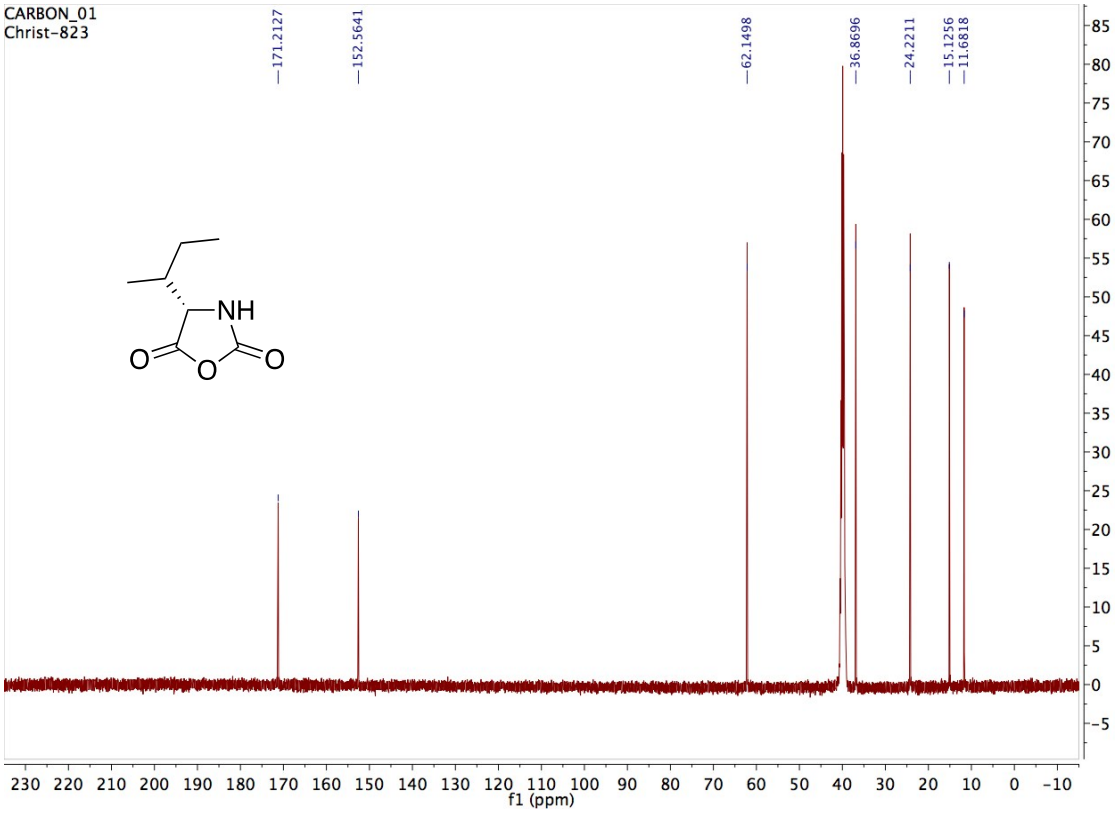

^{1}H-NMR spectrum of L-Alanine *N*-Carboxyanhydride

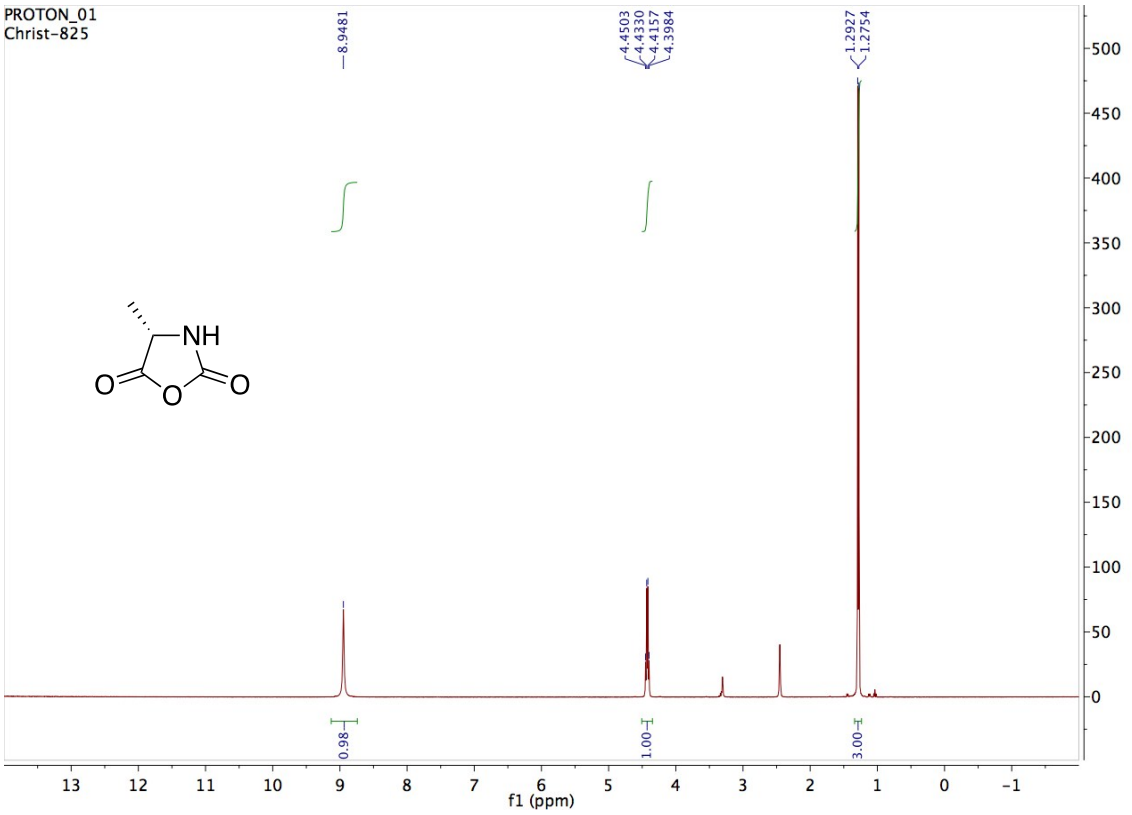

^{1}H-NMR spectrum of L-Alanine *N*-Carboxyanhydride

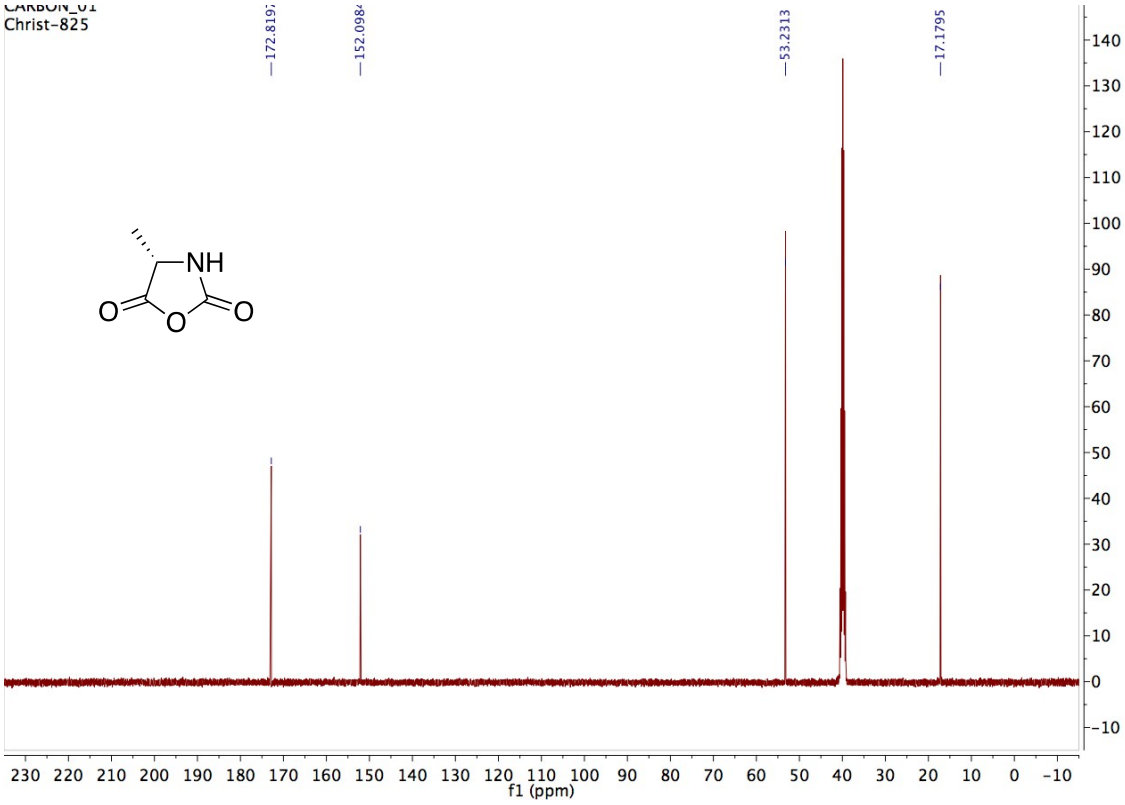

^{1}H-NMR spectrum of L-Valine *N*-Carboxyanhydride

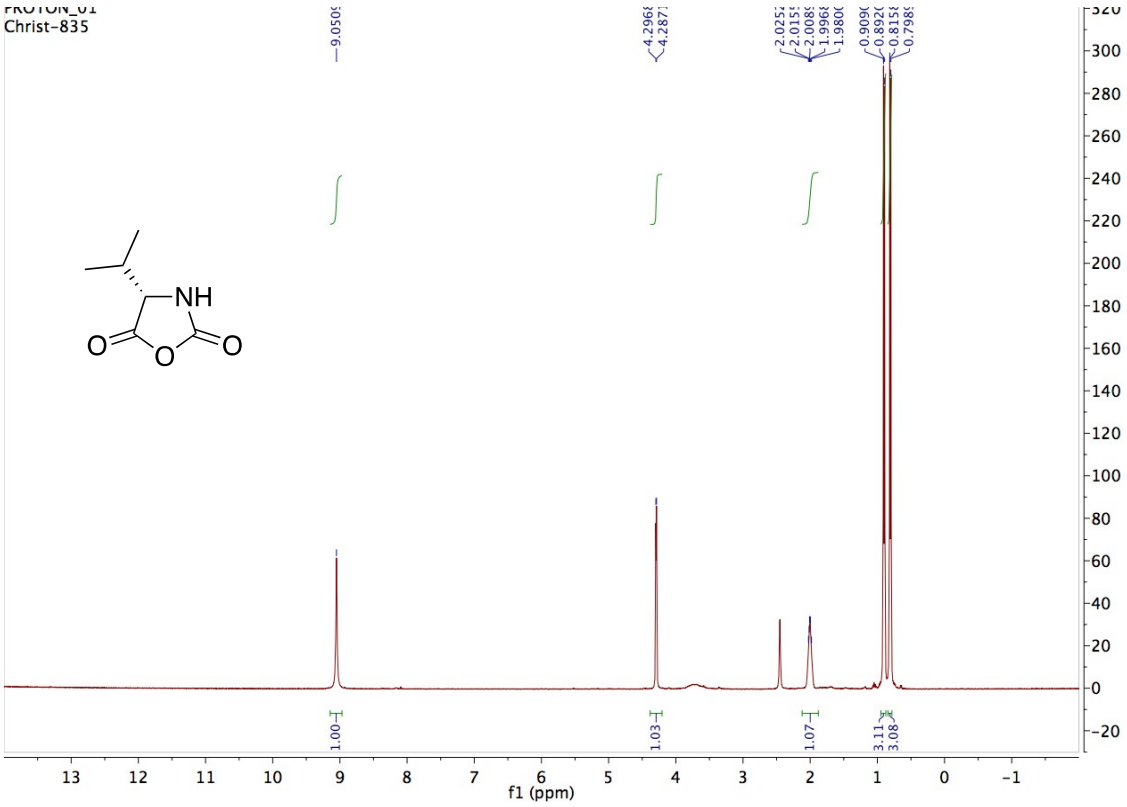

^{1}H-NMR spectrum of L-Valine *N*-Carboxyanhydride

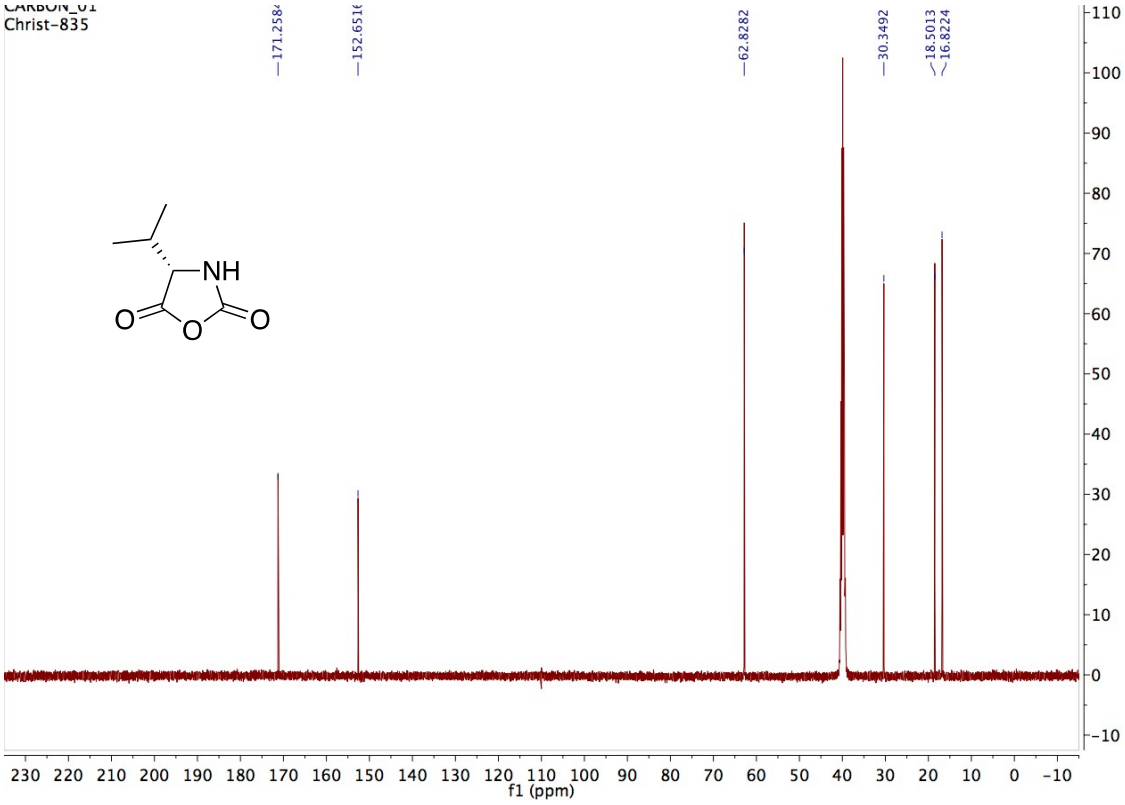

^{1}H-NMR spectrum of 3-(4-naphthalen-2-yl)-1-phenylpro-2-en-1-one

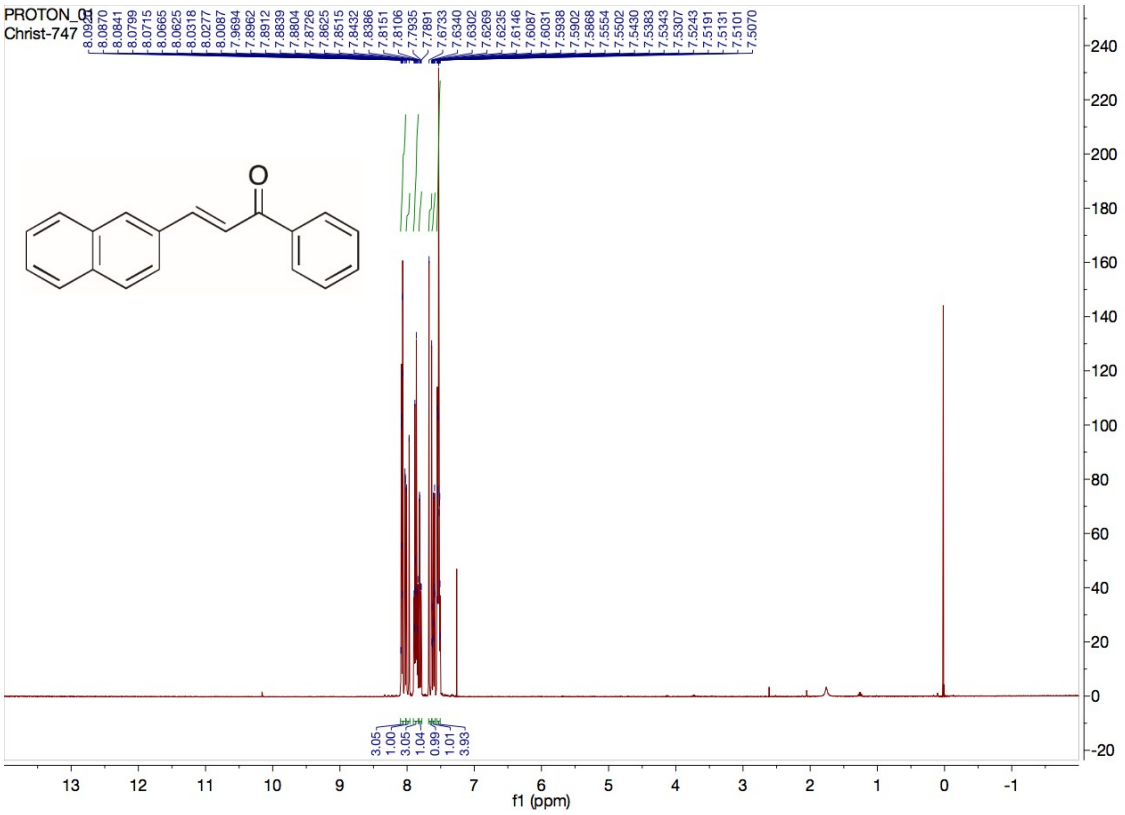

^{13}C-NMR spectrum of 3-(4-naphthalen-2-yl)-1-phenylpro-2-en-1-one

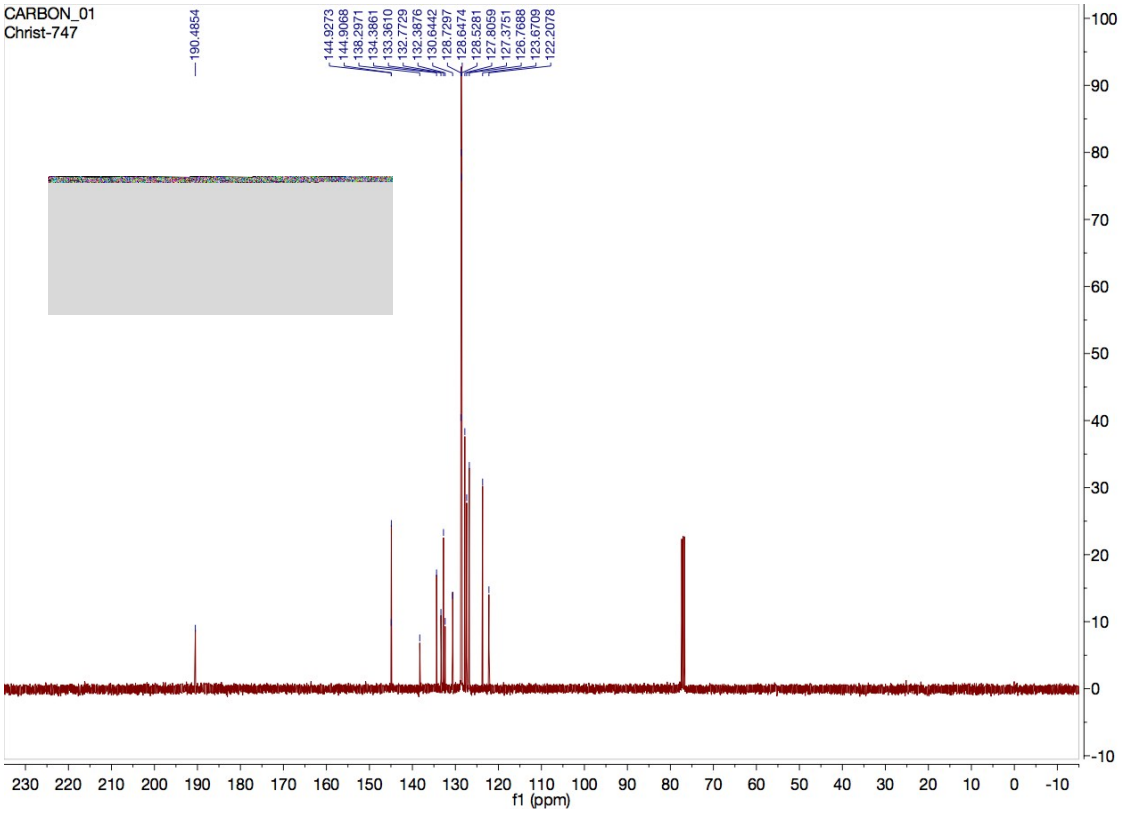

^{1}H-NMR spectrum of 3-(4-trifuoromethylphenyl)-1-phenylpro-2-en-1-one

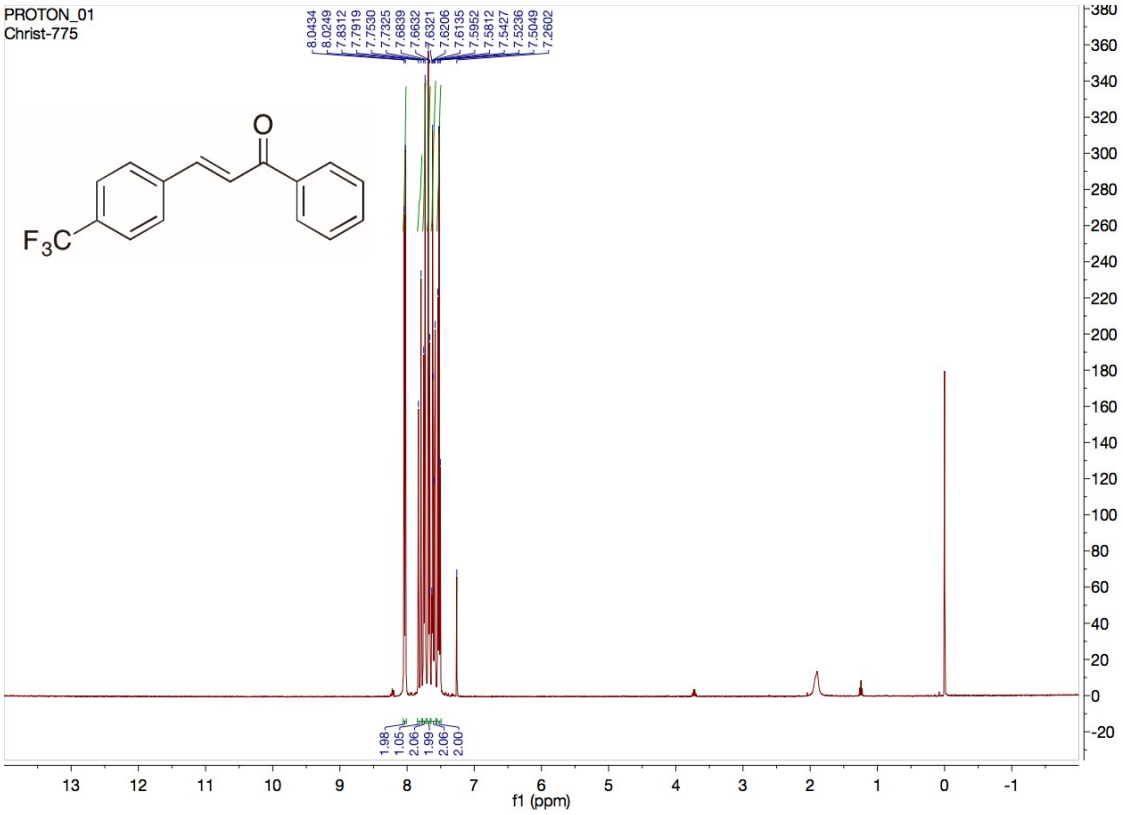

^{13}C-NMR spectrum of 3-(4-trifuoromethylphenyl)-1-phenylpro-2-en-1-one

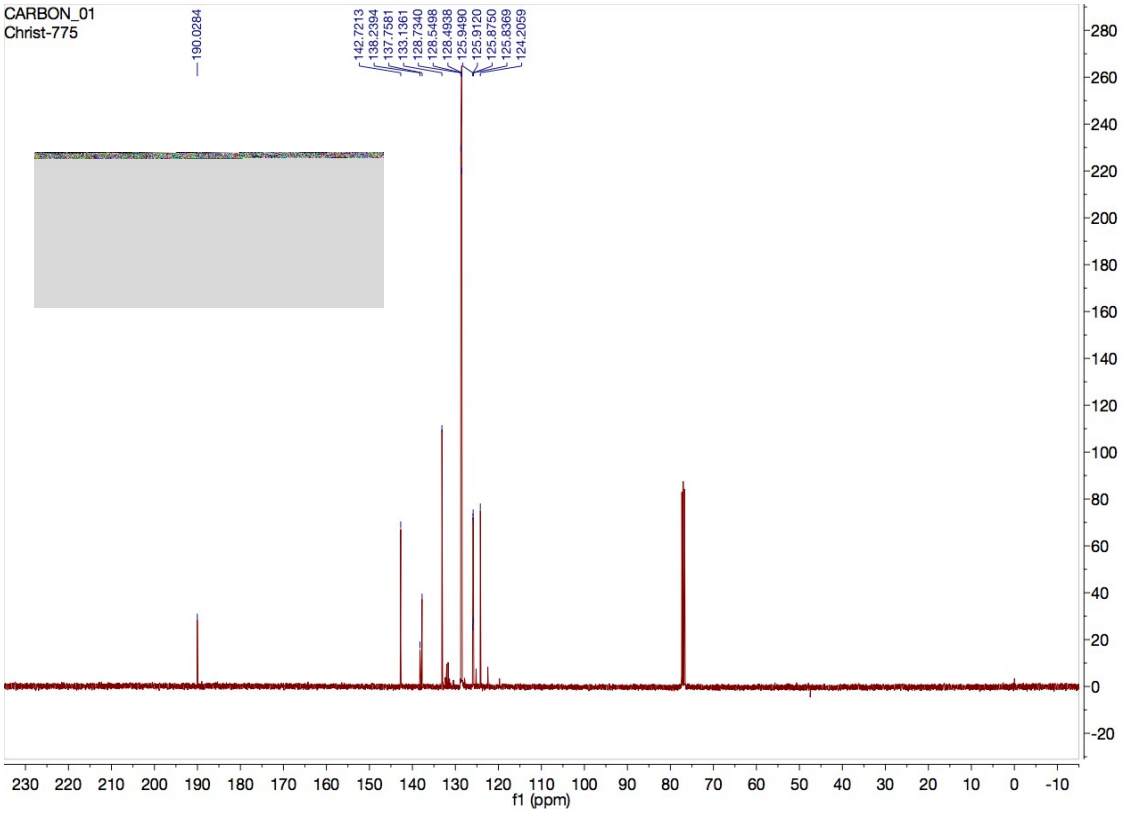

^{19}F-NMR spectrum of 3-(4-trifuoromethylphenyl)-1-phenylpro-2-en-1-one

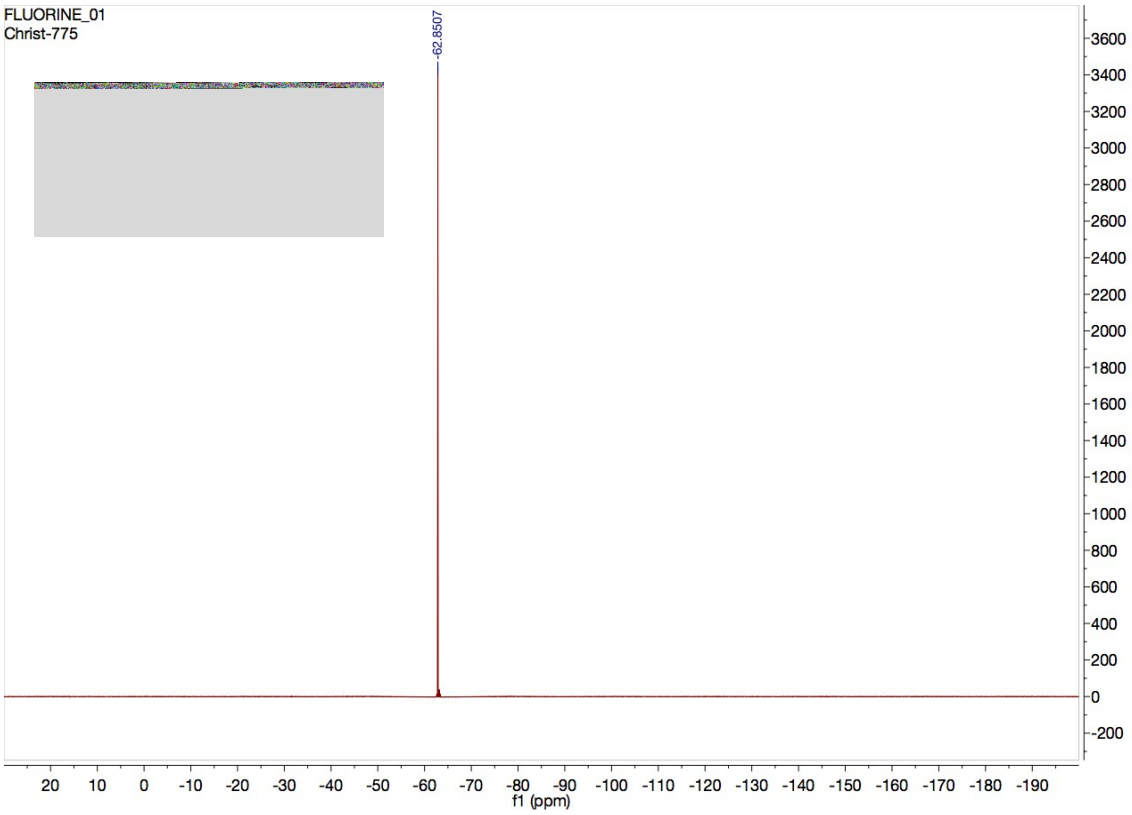

^{1}H-NMR spectrum of *trans*-(*2R,3S*)-Epoxy-1,3-diphenylpropan-1-one (*2a*)[2]

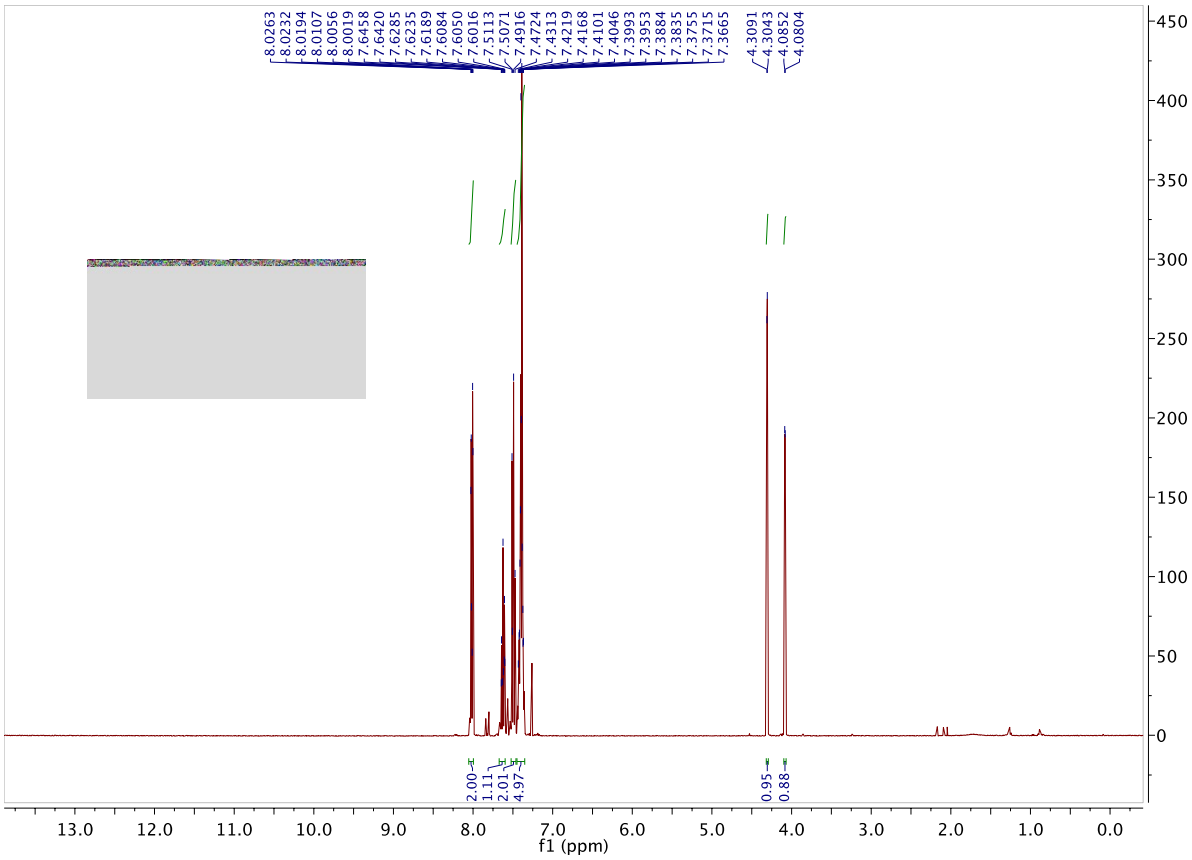

^{13}C-NMR spectrum of *trans*-(*2R,3S*)-Epoxy-1,3-diphenylpropan-1-one (*2a*)

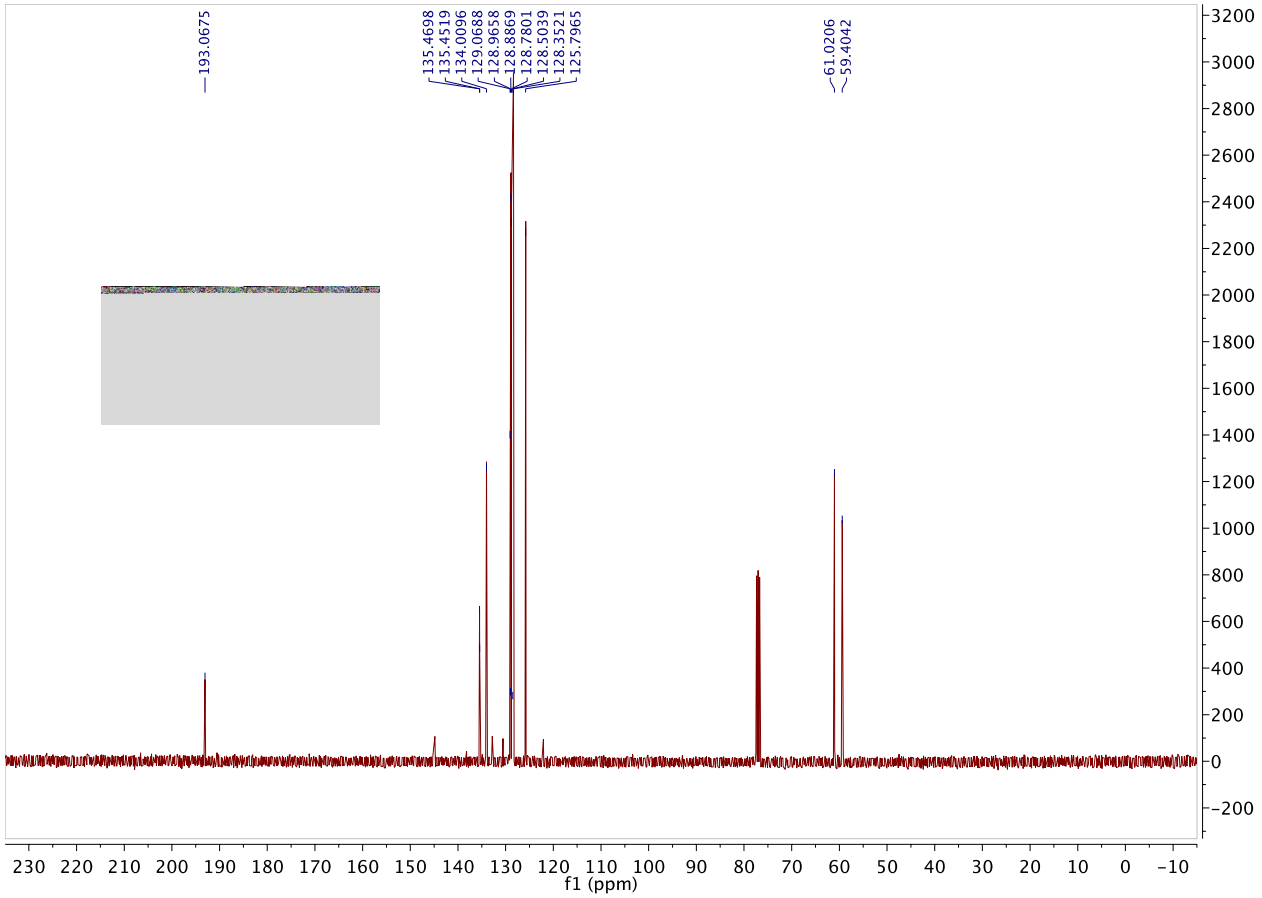

Molecular dynamics simulations

*Trans-chalcone **1** parameterization*. *Trans*-chalcone **1** molecule was built in MOE (www.chemcomp.com). Parameter developpement of the chalcone molecule were previously described.[13] Briefly, initial parameters for the CHARMM general force field (CGenFF v 3.0.1),[14] were automatically assigned using the CGenFF paramchem web server.[15] Parameters for charges, angles and dihedral angles with paramchem penalties above 10 were further optimized using the Force Field Toolkit[16] implemented in VMD 1.9.2.[17] All necessary quantum mechanical calculations for this parameterization were achieved using Gaussian 03.[18]

System preparation. Poly-L-Leucine (PLL) (20-mer) and Poly-L-Alanine (PLA) (20-mer) were built in MOE with an initial α-helix conformation and prepared for molecular dynamics (MD) simulations using the automatic psf builder in VMD.[17] Two systems were built: one composed of the PLL with one chalcone molecule, and the second included the PLA with one chalcone molecule. In both cases, the *trans*-chalcone **1** molecule was placed randomly at a distance of 10 Å of each homo-oligopeptide prior to solvation, leading to systems of 14127 and 15945 atoms for PLA and PLL, respectively.

Simulations. All the MD simulations were performed using NAMD 2.9 using the CHARMM36[19] force field, TIP3 waters[20] periodic boundary conditions and a timestep of 2 fs for long-range electrostatic and 1 fs for all other potentials. The cutoffs for the short-range electrostatic and the Lennard-Jones interactions were 12 Å with the latter smoothed via a switching function over the range of 10 to 12 Å. Long-range electrostatic were calculated via the Particle Mesh Ewald (PME) method[21] using a fourth-order interpolation and a grid spacing of ~1 Å. NPT ensembles were generated. Langevin damping with a coefficient of ps^{-1} was used to maintain a constant temperature of 25 ^{o}C, and the pressure was controlled by a Nosé-Hoover Langevin piston at 1 atm. The length of the bonds between hydrogen and heavy atoms were constrained using the SETTLE[22] for water molecules, and SHAKE[23] for all other molecules. The x-y plane area was kept constant allowing fluctuations of the z axis. Nonbonded pair lists were updated every 10 steps. The

systems were minimized for 300 steps and simulated for 50 ns. The coordinates were saved every 100 ps for analysis.

Trajectory analysis. Nonpolar contacts were characterized between the PLL and *trans*-chalcone **1** using the *measure contacts* command in VMD with a cutoff of 4.5 Å between the heavy atoms. Solvent accessible surface area (SASA) was calculated for *trans*-chalcone **1** using the *measure* function in VMD with a radius (*srad*) of 1.4 A. The orientation adopted by the *trans*-chalcone **1** relatively to the orientation of the PLL alpha-helix was calculated from the dot product of two vectors: one on the PLL (V1) formed between centroid of alpha carbons for residues 4, 5, 6, and 7 on one end and residues 14, 15, 16 and 17 on the other, and the other vector was defined by the C and O atoms of the *trans*-chalcone **1** carbonyl function (V2) (see Fig. XA2).

Asymmetric epoxidation Model building. The *trans*-chalcone **1**/PLL supramolecular complex was manually built in Pymol. Four supramolecular complexes were built as follows. Seven leucine residues were positioned in an alpha helix and the *trans*-chalcone **1** molecule was positioned in the hydrophobic groove formed by the side chains of Leu residues similarly to the bound conformation observed in the MD simulations (see figure 3). A peroxide molecule was then positioned to form H-bonds with the *N*-terminal last three residues. Distance and angle between the hydroperoxide anionic oxygen and the enone reactive carbon of *trans*-chalcone **1** were adjusted to 2.5A and 107 degrees (according to the dunitz angle for nucleophilic attack).[24] In addition to this initial supramolecular complex, three other systems were built with alternate *trans*-chalcone 1 orientations. For these systems, the *trans*-chalcone **1** molecule was flipped on itself to adopt the three other available conformation in the groove with respect to the peroxide and the *N*-terminal (see figure 4A, B, C and D). The four supramolecular complexes were then energy minimized without constraints using the PM6-D3H+ method[25] implemented in the GAMESS software.[26] Analysis of the resulting supramolecular complexes showed that only the conformation depicted in figure 4A presented a reactive conformation with respect to the peroxide with a distance of 2.5A and angle of 98 degree close to the dunitz angle.

Potential energy surface (with the PM6-D3H+ method) obtained from a relaxed surface scan of the distance between the hydroperoxide anionic oxygen and the enone reactive carbon confirmed the reactive nature of this conformation.

References

1. I. Karaman, H. Gezegen, M. B. Gürdere, A. Dingil and M. Ceylan, *Chem. Diovers.*, 2010, **7**, 400.
2. Q. Qian, Y. Tan, B. Zhao, T. Feng, Q. Shen and Y. Yao, *Org. Lett.*, 2014, **16**, 4516.
3. P. A. Bentley, W. Kroutil, J. A. Littlechild and S. M. Roberts, *Chirality*, 1997, **9**, 198.
4. W. D. Fuller, M. S. Verlander and M. Goodman, *Biopolymers*, 1976, **15**, 1869.
5. (a) S. Colonna, H. Molinari, S. Banfi, S. Juliá, J. Masana and A. Alvarez, *Tetrahedron*, 1983, **39**, 1635; (b) R. W. Flood, T. P. Geller, S. A. Petty, S. M. Roberts, J. Skidmore and M. Volk, *Org. Lett.*, 2001, **3**, 683; (c) A. Berkessel, N. Gasch, K. Glaubitz and C. Koch, *Org. Lett.*, 2001, **3**, 3839; (d) R. Takagi, T. Manabe, A. Shiraki, A. Yoneshige, Y. Hiraga, S. Kojima and K. Ohkata, *Bull. Chem. Soc. Jpn.*, 2000, **73**, 2115; (e) R. Takagi, A. Shiraki, T. Manabe, S. Kojima and K. Ohkata, *Chem. Lett.*, 2000, **29**, 366.
6. (a) G. D. Fasman, M. Idelson and E. R. Blout, *J. Am. Chem. Soc.*, 1961, **83**, 709; (b) R. Katakai and Y. Nakayama, *J. Chem. Soc., Chem. Commun.*, 1977, 924; (c) M. Narita, M. Doi, H. Sugasawa and K. Ishikawa, *Bull. Chem. Soc. Jpn.*, 1985, **58**, 1473; (d) M. Narita, K. Ishikawa, H. Sugasawa and M. Doi, *Bull. Chem. Soc. Jpn.*, 1985, **58**, 1731; (e) L. K. Tamm and S. A. Tatulian, *Quart. Rev. Biophys.*, 1997, **30**, 365; (f) S. A. Tatulian, *Biochemistry*, 2003, **42**, 11898.
7. (a) J. Lu, Y.-H. Xu, F. Liu and T.-P. Loh, *Tetrahedron. Lett.*, 2008, **49**, 6007; (b) C. Bérubé and N. Voyer, *Synth. Commun.*, 2016, **46**, 395.
8. Y. Demizu, N. Yamagata, S. Nagoya, Y. Sato, M. Doi, M. Tanaka, K. Nagasawa, H. Okuda and M. Kurihara, *Tetrahedron*, 2011, **67**, 6155.
9. W. Luo, Z. Yu, W. Qiu, F. Yang, X. Liu and J. Tang, *Tetrahedron*, 2011, **67**, 5289.
10. C. Zeng, D. Yuan, B. Zhao and Y. Yao, *Org. Lett.*, 2015, **17**, 2242.
11. B. Wang, C. Miao, S. Wang, C. G. Xia and W. Sun, *Chem. Eur. J.*, 2012, **18**, 6750.
12. S. Juliá, J. Masana and J. C. Vega, *Angew. Chem., Int. Ed. Engl.*, 1980, **19**, 929.
13. C. Bérubé, X. Barbeau, S. Cardinal, B. P.L, C. Bouchard, N. Delcey, P. Lagüe and N. Voyer, 2016, DOI: 10.1080/10610278.2016.1236197.
14. (a) K. Vanommeslaeghe, E. Hatcher, C. Acharya, S. Kundu, S. Zhong, J. Shim, E. Darian, O. Guvench, P. Lopes, I. Vorobyov and A. D. Mackerell, *J. Comput. Chem.*, 2010, **31**, 671; (b) W. Yu, X. He, K. Vanommeslaeghe and A. D. Mackerell, *J. Comput. Chem.*, 2012, **33**, 2451.
15. (a) K. Vanommeslaeghe and A. D. MacKerell, *J. Chem. Inf. Model.*, 2012, **52**, 3144; (b) K. Vanommeslaeghe, E. P. Raman and A. D. MacKerell, *J. Chem. Inf. Model.*, 2012, **52**, 3155.
16. C. G. Mayne, J. Saam, K. Schulten, E. Tajkhorshid and J. C. Gumbart, *J. Comput. Chem.*, 2013, **34**, 2757.
17. W. Humphrey, A. Dalke and K. Schulten, *J. Mol. Graphics*, 1996, **14**, 33.
18. M. J. Frisch, G. W. Trucks, H. B. Schlegel, G. E. Scuseria, M. A. Robb, J. R. Cheeseman, J. A. Montgomery, T. Vreven, K. N. Kudin, J. C. Burant, J. M. Millam, S. S. Iyengar, J. Tomasi, V. Barone, B. Mennucci, M. Cossi, G. Scalmani, N. Rega, G. A. Petersson, H. Nakatsuji, M. Hada, M. Ehara, K. Toyota, R. Fukuda, J. Hasegawa, M. Ishida, T. Nakajima, Y. Honda, O. Kitao, H. Nakai, M. Klene, X. Li, J. E. Knox, H. P. Hratchian, J. B. Cross, V. Bakken, C. Adamo, J. Jaramillo, R. Gomperts, R. E. Stratmann, O. Yazyev, A. J. Austin, R. Cammi, C. Pomelli, J. W. Ochterski, P. Y. Ayala, K. Morokuma, G. A. Voth, P. Salvador, J. J. Dannenberg, V. G. Zakrzewski, S. Dapprich, A. D. Daniels, M. C. Strain, O. Farkas, D. K. Malick, A. D. Rabuck, K. Raghavachari, J. B. Foresman, J. V. Ortiz, Q. Cui, A. G. Baboul, S. Clifford, J. Cioslowski, B. B. Stefanov, G. Liu, A. Liashenko, P. Piskorz, I. Komaromi, R. L. Martin, D. J. Fox, T. Keith, A. Laham, C. Y. Peng, A. Nanayakkara, M. Challacombe, P. M. W. Gill, B. Johnson, W. Chen, M. W. Wong, C. Gonzalez and J. A. Pople, *Journal*, 2003, Gaussian.

19. J. Huang and A. D. Mackerell, *J. Comput. Chem.*, 2013, **34**, 2135.
20. (a) W. L. Jorgensen, J. Chandrasekhar, J. D. Madura, R. W. Impey and M. L. Klein, *J. Chem. Phys.*, 1983, **79**, 926; (b) S. R. Durell, B. R. Brooks and A. Ben-Naim, *J. Phys. Chem.*, 1994, **98**, 2198.
21. (a) T. Darden, D. York and L. Pedersen, *J. Chem. Phys.*, 1993, **98**, 10089; (b) U. Essmann, L. Perera, M. L. Berkowitz, T. Darden, H. Lee and L. G. Pedersen, *J. Chem. Phys.*, 1995, **103**, 8577.
22. S. Miyamoto and P. A. Kollman, *J. Comput. Chem.*, 1992, **13**, 952.
23. J.-P. Ryckaert, G. Ciccotti and H. J. C. Berendsen, *J. Comput. Phys.*, 1977, **23**, 327.
24. H. B. Bürgi, J. D. Dunitz, J. M. Lehn and G. Wipff, *Tetrahedron*, 1974, **30**, 1563.
25. J. C. Kromann, A. S. Christensen, C. Steinmann, M. Korth and J. H. Jensen, *PeerJ*, 2014, **2**, e449.
26. M. W. Schmidt, K. K. Baldridge, J. A. Boatz, S. T. Elbert, M. S. Gordon, J. H. Jensen, S. Koseki, N. Matsunaga, K. A. Nguyen, S. Su, T. L. Windus, M. Dupuis and J. A. Montgomery, *J. Comput. Chem.*, 1993, **14**, 1347.